Petrology of the Chilliwack batholith, North Cascades, Washington: generation of calc-alkaline granitoids by melting of mafic lower crust with variable water fugacity

Jeffrey H. Tepper, * **Bruce K. Nelson, George W. Bergantz, and Anthony J. Irving**

Department of Geological Sciences, AJ-20, University of Washington, Seattle, WA 98195, USA

Abstract. Calc-alkaline granitoid rocks of the Oligocene-Pliocene Chilliwack batholith, North Cascades, range from quartz diorites to granites (57–78% SiO_2), and are coeval with small gabbroic stocks. Modeling of major element, trace element, and isotopic data for granitoid and mafic rocks suggests that: (1) the granitoids were derived from amphibolitic lower crust having REE (rare-earth-element) and Sr-Nd isotopic characteristics of the exposed gabbros; (2) lithologic diversity among the granitoids is primarily the result of variable water fugacity during melting. The main effect of f_{H_2O} variation is to change the relative proportions of plagioclase and amphibole in the residuum. The REE data for intermediate granitoids (quartz diorite–granodiorite; $Eu/Eu^* = 0.84–0.50$) are modeled by melting with $f_{H_2O} < 1$ kbar, leaving a plagioclase + pyroxene residuum. In contrast, data for leucocratic granitoids (leuco-granodiorites and granites; $Eu/Eu^* = 1.0–0.54$) require residual amphibole in the source and are modeled by melting with $f_{H_2O} = 2–3$ kbar. Consistent with this model, isotopic data for the granitoids show no systematic variation with rock type ($^{87}Sr/^{86}Sr_i = 0.7033–0.7043$; $\varepsilon Nd(0) = +3.3$ to $+5.5$) and overlap significantly with data for the gabbroic rocks ($^{87}Sr/^{86}Sr_i = 0.7034–0.7040$; $\varepsilon Nd(0) = +3.3$ to $+6.9$). The f_{H_2O} variations during melting may reflect additions of H_2O to the lower crust from crystallizing basaltic magmas having a range of H_2O contents; Chilliwack gabbros document the existence of such basalts. One-dimensional conductive heat transfer calculations indicate that underplating of basaltic magmas can provide the heat required for large-scale melting of amphibolitic lower crust, provided that ambient wallrock temperatures exceed 800°C. Based on lithologic and geochemical similarities, this model may be applicable to other Cordilleran batholiths.

Introduction

Granitoid batholiths are an important component of continental crust, and their origin has been a central question in petrology for more than two centuries. Debate in recent years has focused on the relative importance of fractional crystallization versus crustal anatexis, and on the role of open system processes such as magma mixing and assimilation. Models for continental arc granitoids commonly assign a fundamental role to mantle-derived mafic magmas. They may be parental magmas (LeBel et al. 1985), end members in mixing or assimilation processes (Reid et al. 1983; DePaolo 1981), material for lower crustal source regions (Gromet and Silver 1987), and/or heat sources that drive crustal melting (Pitcher 1987). Despite the probable importance of basaltic magmas in granitoid genesis, mafic rocks have been overlooked in most studies of arc plutonism. However, gabbros are an integral component of I-type batholiths (Pitcher 1987), and represent mantle-derived magmas that were present during batholith formation. An objective of this study is to determine the relationship between the granitoids and associated gabbros of the Chilliwack batholith, North Cascades, and thereby gain a better understanding of the role of basaltic magmas in granitoid genesis at continental margins.

Petrologic diversity (gabbro to granite) is a characteristic feature of I-type granitoid batholiths. This could be a result of fractional crystallization (Eggins and Hensen 1987), magma mixing (Kistler et al. 1986), restite unmixing (Chappell et al. 1987), wallrock assimilation (DePaolo 1981), source heterogeneity (Noyes et al. 1983), or some combination thereof. Previous studies of Cordilleran granitoids include detailed investigations of differentiation processes operative within individual magma bodies (Hill 1988), as well as large-scale studies that document the influence of regional variations in the age and composition of the lower crust (Farmer and DePaolo 1983). There have been fewer attempts, however, to look at the origins of diversity among different intrusions within the same batholith, and that is the second objective of this study. The Chilliwack is well suited for this purpose because it contains a wide range of pluton types (gabbro to granite)

* *Present address:* Department of Geology, Union College, Schenectady, NY 12308, USA
Correspondence to: J. Tepper

that were emplaced within a limited range of time (< 35 Ma) and space (< 1,000 km^2). This is one of the first detailed studies of Cascade arc plutonism. Petrologic similarities between Chilliwack granitoids and those in California and South America suggest the results of this study may be applicable to other continental arc batholiths.

Geologic setting and rock types

Cascade arc magmatism is related to subduction of the Juan de Fuca plate beneath western North America. In the southern and central Cascades magmatism is represented by calc-alkaline volcanic rocks, but in the North Cascades Plio-Pleistocene uplift has led to erosion of the volcanic cover and exposure of a chain of epizonal batholiths. The largest of these is the 960 km^2 Chilliwack batholith (Fig. 1), which contains dozens of individual plutons that were emplaced between 34–2 Ma into a diverse assemblage of pre-Tertiary metamorphic rocks and subordinate Tertiary volcanic and sedimentary rocks (Misch 1966). Rock types in the Chilliwack range from gabbro to granite, but the most abundant lithologies are granodiorite, tonalite, and quartz diorite.

Mafic plutons comprise approximately two percent of the outcrop area, and overlap in age with the granitoids (Tepper 1991). On a local scale within the batholith, however, field relations indicate the mafic stocks predate the adjacent granitoids. These small (< 5 km^2), lithologically diverse gabbros and diorites are plutonic equivalents of calc-alkaline and tholeiitic lavas erupted elsewhere in the Cascades, and may be subdivided on the basis of mineral assemblage and chemical composition into a medium-K series (MKS) and a low-K series (LKS). The MKS includes pyroxene gabbros, diorites, and quartz diorites, and is the more widespread series. These rocks probably crystallized from high-alumina basaltic magmas, and are similar to mafic plutons in other Cordilleran batholiths (c.f., Erickson 1977; Walawender and Smith 1980). The LKS rocks are less abundant; they range from gabbro through quartz diorite and are interpreted as having crystallized from high-alumina tholeiitic basalts. Both LKS and MKS plutons are typically composite, consisting of several pulses that show a progression, with decreasing age, toward more differentiated compositions. Chemical variation among pulses (gabbro-diorite-quartz diorite) is modeled by fractional crystallization, accompanied in some cases by minor wallrock assimilation. The petrology of the mafic plutons will be discussed in detail in a separate paper.
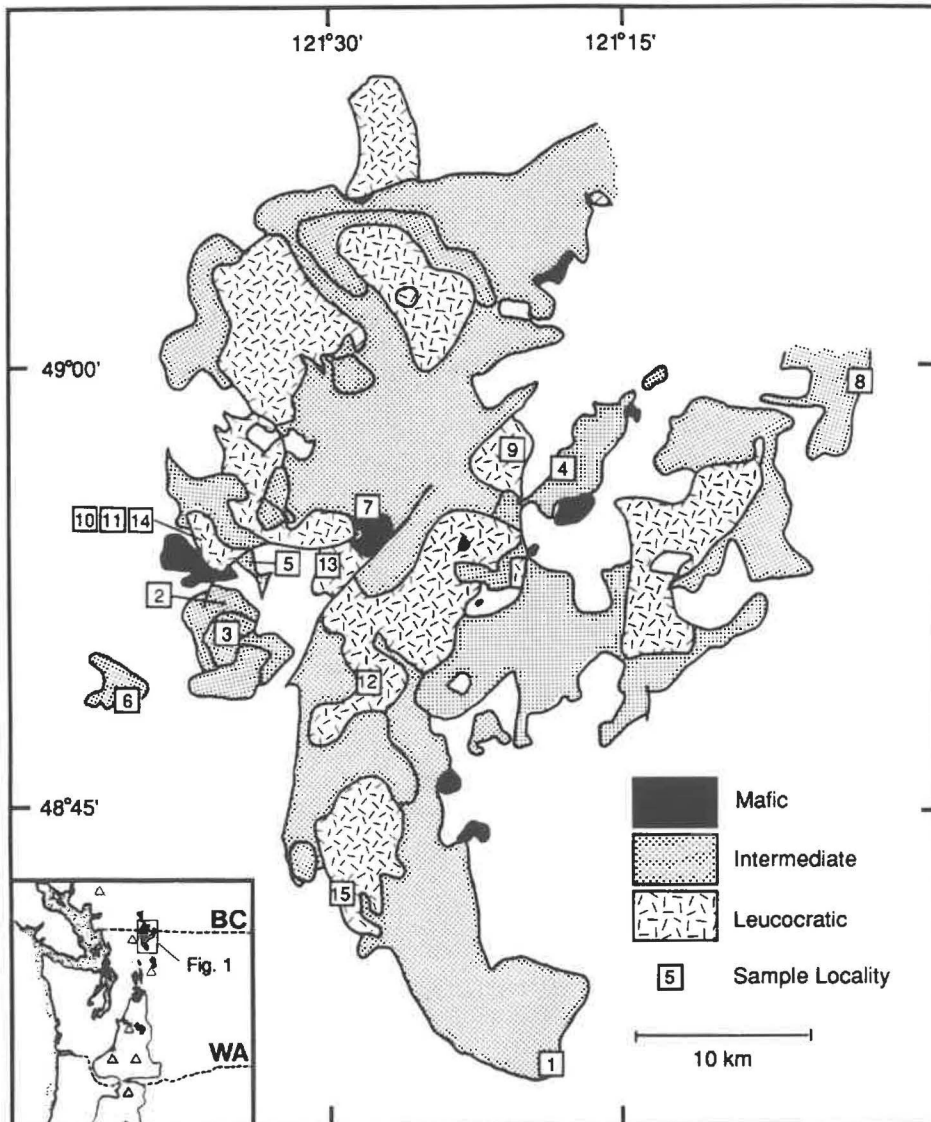

Fig. 1. Simplified geologic map of the Chilliwack batholith compiled from Richards (1971), Tepper (1991) and Tabor and Haugerud (U.S Geological Survey, written communication). Sample numbers refer to granitoid analyses in Table 2. *Inset* shows location of the Chilliwack batholith in relation to volcanic, *gray*, and plutonic, *black*, rocks of the Cascade arc
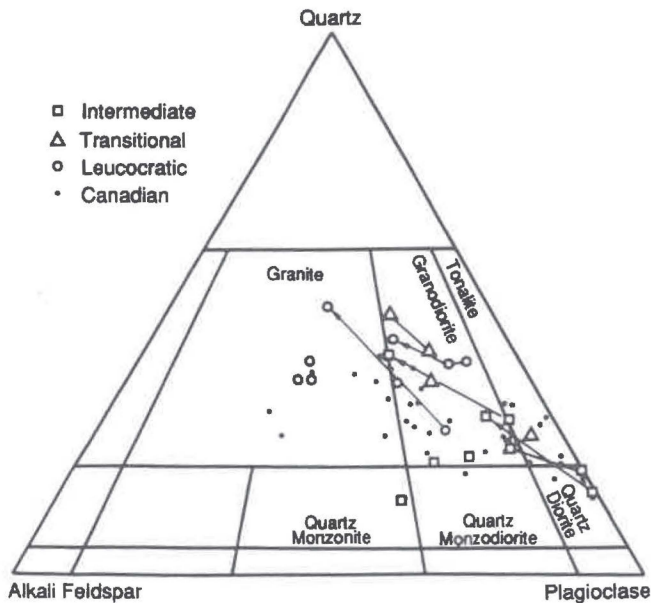
Fig. 2. IUGS classification of Chilliwack granitoids (LeMaitre 1989). Tie lines connect samples from the same pluton, illustrating zoning. Data for Canadian samples from Richards (1971); other data from Table 2 and Tepper (1991)

Table 1. Comparison of granitoid groups

	Intermediate	Transitional	Leucocratic
Rock types:	Granodiorite Tonalite Quartz diorite Quartz monozonite	Granodiorite Tonalite	Granodiorite Granite
Relative area:	67%	---------31%---------	
Mafic mineral assemblage:	Hornblende + biotite + augite $\pm$ hypersthene	Biotite + hornblende $\pm$ hypersthene	Biotite $\pm$ hornblende
Color index:	29–11	10–6	7–2
SiO_2 (wt%):	57.7–66.1	65.8–71.5	64.4–74.0
MgO (wt%):	3.98–2.22	2.05–1.18	1.69–0.57
$Mg/(Mg + Fe^*)$:	0.54–0.45	0.49–0.47	0.42–0.37
$(Eu/Eu^*)_N$:	0.84–0.50	0.73–0.53	1.01–0.54
$(Dy/Lu)_N$:	1.14–1.29	0.85–0.97	0.82–0.92

Chemical and isotopic compositions of the granitoids

Fifteen samples that represent the range of granitoid rock types present in the batholith were chosen for major and trace element analysis; analytical methods are in Appendix I. The samples range from 57–78% SiO_2 (Table 2). On Harker plots (Fig. 3) they overlap with the more differentiated samples from the mafic plutons, but the granitoids show less scatter, particularly in Al_2O_3, FeO, MgO, and CaO contents. This probably reflects less crystal accumulation in the granitoid samples, whereas some mafic samples were clearly enriched in plagioclase or pyroxene. No gaps between intermediate and leucocratic samples are apparent on these variation diagrams. However, if aplites (82-075, R-212) are excluded, the leucocratic rocks differ from the intermediate rocks in having lower MgO contents and lower Mg-numbers [$Mg/(Mg + Fe_{total})$] (Table 1). At equal SiO_2, the leucocratic samples also have higher Al_2O_3 and Na_2O contents (Fig. 3).

The leucocratic plutons generally have lower levels of compatible trace elements (Ni, Cr, Sc, V, Sr, Y) and higher levels of Ba than the intermediate plutons (Table 2), but the distinction between the two groups is most apparent from contrasts in their chondrite-normalised (N) REE patterns (Fig. 4). Intermediate samples are moderately L(light)REE enriched ($La_N/Yb_N = 3.7$–4.5; $La_N/Nd_N = 1.4$–2.0), and have negative Eu anomalies [$(Eu/Eu^*)_N = 0.84 - 0.50$]. In contrast, the leucocratic rocks have distinctive concave upward REE patterns ($Dy_N < Lu_N$), more fractionated LREE ($La_N/Nd_N = 2.3$–3.1), and $(Eu/Eu^*)_N$ ranging from 1.0–0.54. Samples from transitional plutons display some REE characteristics of the intermediate samples [$La_N/Nd_N = 1.8$–1.9 and $(Eu/Eu^*)_N = 0.73$–0.53], but also show the concave upward pattern of the leucocratic sample ($Dy_N < Lu_N$). Among samples *within* each of these three groups, absolute REE abundances and negative Eu anomalies tend to increase with SiO_2 content, but the shapes of the REE patterns remain similar. It is also important to note that samples from the same pluton have similar REE patterns, even in the case of zoned plutons (82-028, 82-063).

Compared to the mafic stocks, granitoid plutons in the Chilliwack are larger (some > 100 km²) and, at the outcrop scale, less heterogeneous. All are I-types (Chappell and White 1974), and range from quartz diorite through granite (Fig. 2). The granitoids may be subdivided into two main groups: (1) *intermediate plutons* (granodiorite, tonalite, and quartz diorite); (2) *leucocratic plutons* (leucocratic granodiorite and granite). A few plutons have some characteristics of both groups, and are referred to *transitional plutons*. Among these three groups the most obvious contrasts are in color index, mafic mineral assemblage, and REE (rare-earth-element) pattern (Table 1). Ages of leucocratic plutons cluster within two intervals, 26–33 Ma and 8–9 Ma, whereas dates on intermediate plutons span the range 2–34 Ma (Tepper 1991). No other patterns are apparent in the spatial or temporal distribution of granitoids of the three groups.

Intermediate plutons make up about 67% of the Chilliwack batholith, and are commonly zoned from quartz diorite or tonalite at the margins to granodiorite in the interior (Fig. 2). They are generally medium grained, equigranular, and hypidiomorphic, with 50–70% plagioclase, 5–12% each hornblende and biotite, 10–20% quartz, and up to 15% orthoclase. Plagioclase (An_{70-16}) is the earliest-formed mineral and in many cases is complexly zoned. Magnesio-hornblende, which formed late in the crystallization history, is subhedral to anhedral and commonly contains cores of relict augite or hypersthene. Biotite, quartz, and alkali feldspar occur predominantly as interstitial phases. Accessory minerals include opaque oxides, apatite, zircon, and rare monazite and allanite.

Leucocratic rocks account for approximately 31% of the batholith. They occur as discrete intrusions, readily distinguished from the felsic portions of intermediate plutons which have higher color indices and different chemical traits (Table 1). Some leucocratic plutons are zoned (Fig. 2), but at the outcrop scale they appear homogeneous. They are typically medium grained and hypidiomorphic. Plagioclase displays oscillatory-normal zoning (An_{48-10}; calcic cores (up to An_{60}) are rare. Biotite (1–6%) is commonly the only mafic mineral, although minor hornblende (< 5%) is also present in a few sections. Orthoclase is interstitial and may form graphic intergrowths with quartz. Accessory minerals are scarce, but include opaque oxides, apatite, zircon, and rare sphene and monazite.

Table 2. Major and trace element, and modal data for Chilliwack granitoids

	1	2	3	4	5	6	7	8
Field no.	87-001	82-028	82-063	RWT500-66	82-135	88-061	88-028	88-020
Rock type	Intermediate Qtz diorite	Intermediate Granodiorite	Intermediate Granodiorite	Intermediate Qtz monzonite	Intermediate Granodiorite	Intermediate Granodiorite	Transitional Tonalite	Transitional Granodiorite
SiO_2	57.64	57.03	66.09	62.11	62.31	62.82	65.87	69.20
TiO_2	0.79	0.84	0.54	0.83	0.66	0.94	0.41	0.35
Al_2O_3	17.42	17.19	15.19	15.91	16.37	15.79	16.23	14.80
Fe_2O_3[a]	6.65	1.79	1.52	5.37	1.62	5.90	4.30	3.27
FeO		4.74	2.91		3.45			
MgO	3.91	3.96	2.22	2.39	3.08	2.45	2.05	1.49
MnO	0.12	0.11	0.09	0.08	0.09	0.10	0.09	0.07
CaO	6.86	7.17	4.07	4.61	5.67	4.76	3.94	3.09
Na_2O	3.69	3.55	3.30	4.05	4.28	4.22	3.83	3.58
K_2O	1.72	2.04	2.72	3.06	1.76	2.49	2.28	3.00
P_2O_5	0.20	0.21	0.17	0.20	0.19	0.23	0.12	0.16
LOI[b]	0.38	0.86	1.13	0.65	0.94	0.27	0.28	0.60
Total	99.36	99.46	99.95	99.25	100.42	99.97	99.38	99.59
Mg/(Mg + Fe)	0.54	0.53	0.48	0.47	0.53	0.45	0.49	0.47
Ni	28		28	16	36	14	7	14
Cr	51	42	25	29	32	36	10	20
Sc	19	15	15	13	15	14	11	9
V	171	173	119	115	132	120	87	74
Sr	383	301	260	362	383	403	365	233
Ba	424	382	654	719	652	693	669	782
Rb		55.0		90.2	45.1	64.0	46.9	83.8
Cs	1.17				1.14		1.43	
U					1.1		0.6	
Th					4.1		2.0	
Hf					3.4		3.2	
Pb								
Zn	72	62	50	38	60	64	53	44
Cu	28	42	30	20	32	36	9	17
Nb								
Ta					1.74		0.28	
Y	23.3	23.5	33.2	31.1	24.1	30.6	16.3	29.6
Zr	36	23	95	275	58	268	114	141
Be	1.1		1.7	1.9	1.4	2.2	1.0	1.6
Li	22		26	10	23	14	21	38
Ga								
Sb					0.30		0.05	
La	11.3	14.5	19.8	29.1	16.5	25.0	12.0	16.8
Ce	27.2	34.4	46.2	61.4	34.3	55.9	24.3	37.5
Nd	13.9	20.2	21.3	28.6	15.8	27.3	12.6	17.8
Sm	3.69	3.90	5.39	6.14	3.82	6.45	2.84	4.20
Eu	1.03	0.96	0.86	1.16	0.92	1.23	0.67	0.72
Gd	3.68	4.63	4.89	5.30	3.67	5.52	2.72	3.98
Dy	3.77	4.65	5.30	4.99	3.78	5.73	2.83	4.39
Ho	0.81	0.93	1.14	1.07	0.81	1.10	0.51	0.95
Yb	2.07	2.33	2.93	2.81	2.22	3.16	1.81	2.91
Lu	0.31	0.36	0.44	0.42	0.33	0.50	0.29	0.45
MODES								
Quartz	12.0	20.2	33.0	11.6	17.4	18.4	22.4	31.8
Plagioclase	67.4	45.6	34.0	46.2	48.6	50.2	62.0	53.8
Orthoclase	–	4.8	17.4	26.8	13.2	20.2	4.6	14.0
Clinopyroxene	tr	3.4	0.2	1.6	–	3.4	–	–
Orthopyroxene	–	1.2	–	–	–	–	–	tr
Amphibole	11.6	11.8	6.4	8.8	10.8	3.6	4.0	1.8
Biotite	8.2	11.8	8.6	2.0	9.2	3.4	5.4	7.4
Opaque	0.8	1.2	0.4	1.8	0.8	0.6	1.4	1.2
Accessories	apa, zir	apa, zir	apa	apa, zir	apa, zir	apa	apa, zir	apa, zir

Table 2 (continued)

	9	10	11	12	13	14	15
Field No.	87-098	82-148	82-074	RWT269-87	88-058	82-075	R-212
Rock Type	Transitional Granodiorite	Leucocratic Tonalite	Leucocratic Granodiorite	Leucocratic Granodiorite	Leucocratic Granite	Leucocratic Aplite	Aplite Aplite
SiO_2	71.53	64.40	69.73	73.07	74.01	76.30	77.45
TiO_2	0.29	0.50	0.33	0.25	0.23	0.22	0.05
Al_2O_3	14.59	17.16	15.66	14.30	13.90	12.65	12.78
Fe_2O_3[a]	2.60	1.92	1.37	1.98	1.72	0.09	0.89
FeO		2.35	1.37			0.65	
MgO	1.18	1.69	0.87	0.70	0.57	0.01	0.03
MnO	0.08	0.09	0.07	0.05	0.04	0.01	0.02
CaO	2.83	4.65	2.90	1.79	1.64	0.54	0.45
Na_2O	3.82	4.87	4.72	4.39	4.12	3.74	4.01
K_2O	2.53	1.61	2.11	3.08	3.21	4.95	3.13
P_2O_5	0.09	0.20	0.11	0.09	0.07	0.04	0.03
LOI[b]	0.45	0.71	0.41	0.37	0.48	0.14	0.31
Total	99.99	100.15	99.64	100.06	99.51	99.20	99.14
Mg/(Mg + Fe)	0.47	0.42	0.37	0.41	0.40	0.02	0.06
Ni	4	13	4	3	4	< 3	< 3
Cr	10	12	5	6	4	< 4	< 4
Sc	6	9	5	4	5	2	2
V	51	87	44	24	22	<21	<21
Sr	247	425	279	277	185	16	34
Ba	741	648	848	787	939	52	731
Rb	65.5		56.6	78.5	71.2		101.3
Cs	2.66		1.13		1.40		
U	1.9		1.8		1.8		3.5
Th	5.5		4.0		5.4		7.1
Hf			2.9				
Pb			5.1				10.0
Zn	32	54	34	25	18	2	11
Cu	54	16	4	4	13	< 3	16
Nb			5.5				7.5
Ta			1.62				
Y	24.3	16.2	11.7	13.3	16.8	16.1	27.6
Zr	89	79	101	128	85	47	67
Be	1.1	1.4	1.2	1.8	1.6	2.0	1.4
Li	13	19	24	16	18	< 10	42
Ga			13.6				13.8
Sb			0.11				
La	14.3	15.7	12.5	21.7	18.3	13.2	22.4
Ce	32.5	35.5	23.8	44.3	33.7	26.6	47.3
Nd	14.3	13.2	10.2	13.4	11.8	9.7	18.7
Sm	3.19	2.74	2.05	2.33	2.39	2.06	4.17
Eu	0.59	0.87	0.62	0.54	0.40	0.14	0.28
Gd	3.02	2.42	1.79	1.87	2.06	1.98	3.53
Dy	3.56	2.47	1.78	1.88	2.30	2.57	3.94
Ho	0.81	0.54	0.37	0.44	0.51	0.69	0.89
Yb	2.62	1.65	1.22	1.39	1.70	3.05	2.69
Lu	0.42	0.27	0.21	0.22	0.28	0.52	0.41
MODES							
Quartz	45.4		40.8	34.0	48.0		36.9
Plagioclase	33.4		35.5	41.2	24.0		26.4
Orthoclase	15.4		16.8	21.3	24.4		36.2
Clinopyroxene	–		–	–	–		–
Orthopyroxene	–		–	–	–		–
Amphibole	1.2		–	–	–		–
Biotite	4.2		5.5	3.4	3.2		1.4
Opaque	0.4		0.9	1.0	0.4		tr
Accessories	apa, zir		apa, mona	–	–		zir

Table 2. (continued)

	87-027 Amphibole xenocryst	82-074 Feldspar separate
SiO_2	43.20	
TiO_2	1.63	
Al_2O_3	13.59	
FeO	9.55	0.12
MgO	15.78	
MnO	0.12	
CaO	11.13	3.13
Na_2O	2.21	4.69
K_2O	0.14	1.5
F	0.10	
OH = F	-0.04	
H_2O	2.12	
Total	99.53	
Mg/(Mg + Fe)	0.74	
Ni	270	< 6
Cr	246	0.3
Sc	113	0.1
Sr	190	390
Ba	40	467
Cs	0.19	0.16
U	< 0.6	0.16
Th	< 0.17	0.23
Hf	0.46	0.32
Sb	< 0.16	0.07
La	0.4	4.5
Ce	2.6	5.7
Nd		1.9
Sm	1.57	0.20
Eu	0.74	0.59
Tb	0.39	0.02
Yb	1.43	0.09
Lu	0.18	0.02

Major oxides in weight %; trace elements in parts per million.
[a] Total Fe reported as Fe_2O_3 except for samples in which FeO was analyzed separately. [b] For samples in which FeO was determined separately, LOI (loss on ignition) has been adjusted to remove weight gain due to oxidation of FeO. Modes determined by point counting (500–1,300 points); tr, trace amounts; apa, apatite; zir, zircon; mona, monazite

Isotopic data for Sr and Nd were obtained for 11 granitoid samples (Table 3; analytical details are in Appendix I). No systematic difference exists among initial $^{87}Sr/^{86}Sr$ ratios for intermediate samples (0.7036–0.7042), transitional samples (0.7040–0.7043), and leucocratic samples (0.7033–0.7041). Values of $\varepsilon Nd(0)$ range only between + 3.3 and + 5.5, again with no systematic difference among groups. These compositions overlap significantly with those of Chilliwack gabbros and diorites ($^{87}Sr/^{86}Sr_i$ = 0.7034–0.7040; $\varepsilon Nd(0)$ = + 3.3 to + 6.9) (Tepper 1991).

Petrogenesis of the granitoid rocks

Fractional crystallization and crustal anatexis are two end member processes that may produce granitic magmas, and both probably contributed to generation of the Chilliwack granitoids. However, geochemical data from mafic and granitoid rocks suggest that the petrologic differences between the intermediate and leucocratic plutons result primarily from differences in melting reactions, and that fractional crystallization did not greatly modify the compositions of the granitoid magmas.

Differentiation of mafic magmas

Mafic stocks in the Chilliwack crystallized from basaltic magmas similar in composition to calc-alkaline and tholeiitic arc basalts erupted elsewhere in the Cascades, and as such, represent possible parent magmas for the granitoids. These stocks are typically composite, containing a range of rock types that document the chemical evolution of the basaltic magmas.

Of the two mafic rock series in the Chilliwack, only the MKS may represent granitoid parent magmas. A parental role for LKS magmas is precluded by lower levels of *both* compatible and incompatible trace elements in LKS samples than in the granitoids. For example, the most differentiated LKS sample, a quartz diorite with 12 ppm Rb, would have to undergo a minimum of 75% crystallization (assuming $\bar{D}_{Rb} = 0$) to reach 45 ppm, the Rb content of 82–135, the lowest-Rb granitoid. Assimilation of metasedimentary wallrock could raise Rb levels with less crystallization, but this LKS quartz diorite contains only 2 ppm Ni (versus 35 ppm for 82–135) and no plausible fractional crystallization process, with or without assimilation, can account for a 17-fold *increase* in Ni during differentiation.

Of the MKS stocks, the best studied is the Mt. Sefrit Gabbronorite, which consists of four nested intrusions ranging from olivine gabbronorite through quartz diorite. Mineralogical variations and geochemical modeling suggest these rock types are related by low-pressure crystal fractionation, with the quartz diorite being the product of approximately 50% crystallization of the gabbronorite (Tepper 1991). With differentiation, REE abundances increase and $(Eu/Eu^*)_N$ values decrease, but La_N/Yb_N remains nearly constant (5.8–6.2). The quartz dioritic daughter plutons at Mt. Sefrit are similar in major element composition to intermediate granitoids elsewhere in the Chilliwack, suggesting the possibility that these granitoids also could be differentiates of MKS basalts. However, in addition to being much larger in size, the granitoid plutons have less-fractionated REE patterns (La_N/Yb_N = 3.7–4.5) (Fig. 5), which cannot be produced from an MKS parent magma by fractional crystallization of minerals observed in the MKS plutons or the intermediate granitoids. This argues against the granitoids being differentiates of MKS basalts. In theory, fractionation of allanite or monazite could produce the required decrease in La_N/Yb_N, but that is unlikely in this case because: (1) these minerals are not found in MKS stocks, and are rare in intermediate plutons, generally occurring only in their most differentiated parts; (2) where present both allanite and monazite occur as late-formed interstitial phases, and so probably did not influence early magma evolution; (3) even among the felsic samples that contain these accessory minerals, no decrease in La_N/Yb_N with differentiation is observed. Similarly, apatite fractionation is an unlikely
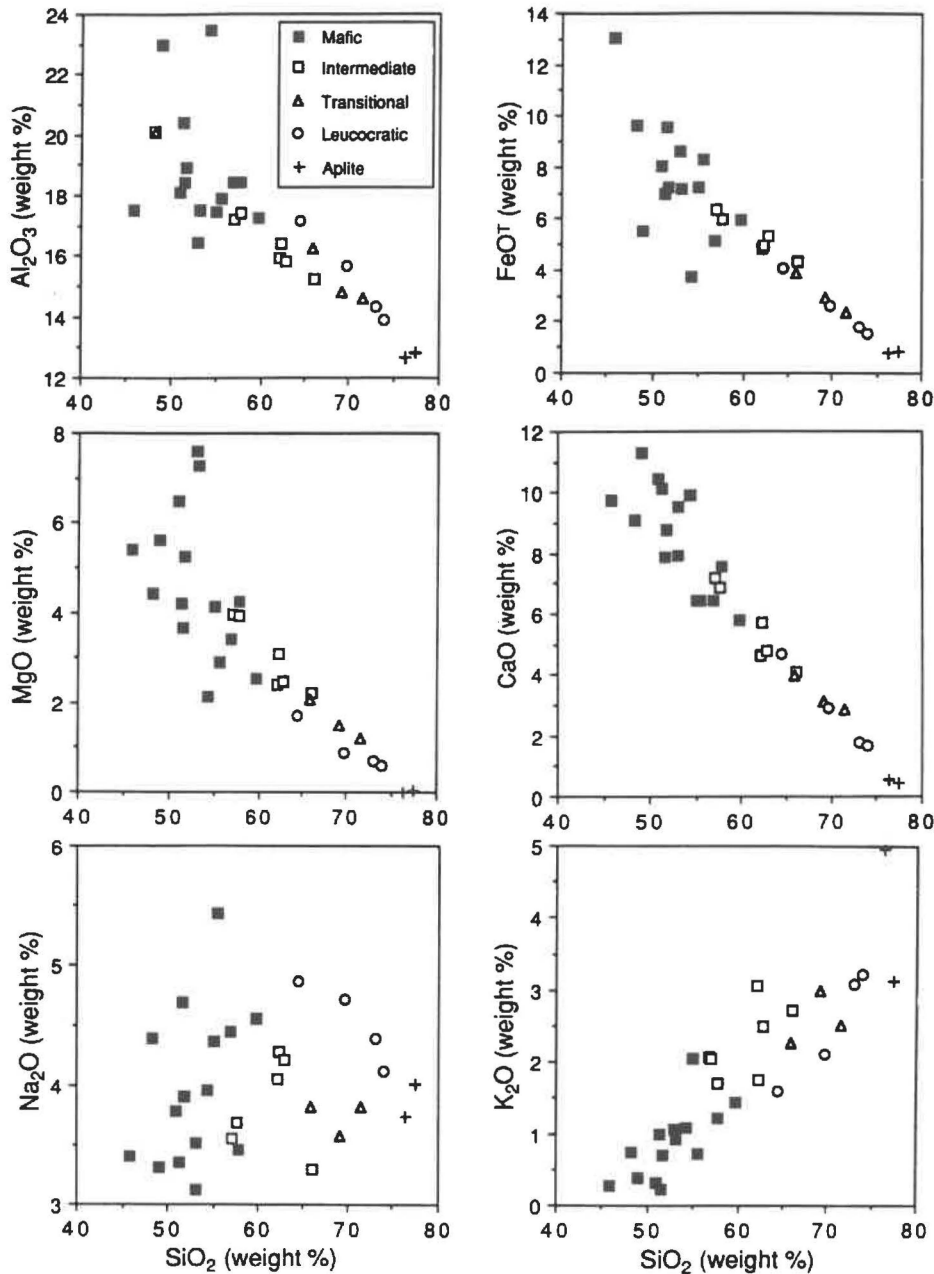
Fig. 3. Harker variation diagrams for 30 mafic and granitoid samples from the Chilliwack batholith. Data from Table 2 (granitoids) and Tepper (1991) (mafic rocks)

means of appreciably lowering La_N/Yb_N because apatite/melt partition coefficients for LREE and H(heavy)REE are not greatly different (Watson and Green 1981). Even if apatite were to account for 2% of the crystals removed, the change in La_N/Yb_N would be < 2%.

Granodiorite 82-074 has a REE pattern representative of the leucocratic granitoids (Fig. 5). The absence of a Eu anomaly in this sample argues against it being a differentiate of a more-mafic magma because all samples from MKS stocks and intermediate granitoids have negative Eu anomalies that become more pronounced with differentiation, and are unlikely to be "erased" during continued crystallization. Fractional crystallization of amphibole and plagioclase together could produce a felsic

magma with a concave upward REE pattern and no Eu anomaly, but we consider this an unlikely explanation for these rocks because it conflicts with results of major element modeling (see below), and because in other studies of arc magmatism (Perfit et al. 1980; Luhr and Carmichael 1980) $(Eu/Eu*)_N$ decreases with differentiation, even when amphibole is involved. There is also no evidence that the absence of a Eu anomaly in the leucocratic samples reflects feldspar accumulation or crystallization at high f_{O_2}. The samples with the highest modal proportions of feldspar are quartz diorites and tonalites, all of which have negative Eu anomalies. Feldspar separated from 82–074 has $(Eu/Eu*)_N = 8.48$ (Table 2), indicating significant Eu^{2+} was present during crystallization.
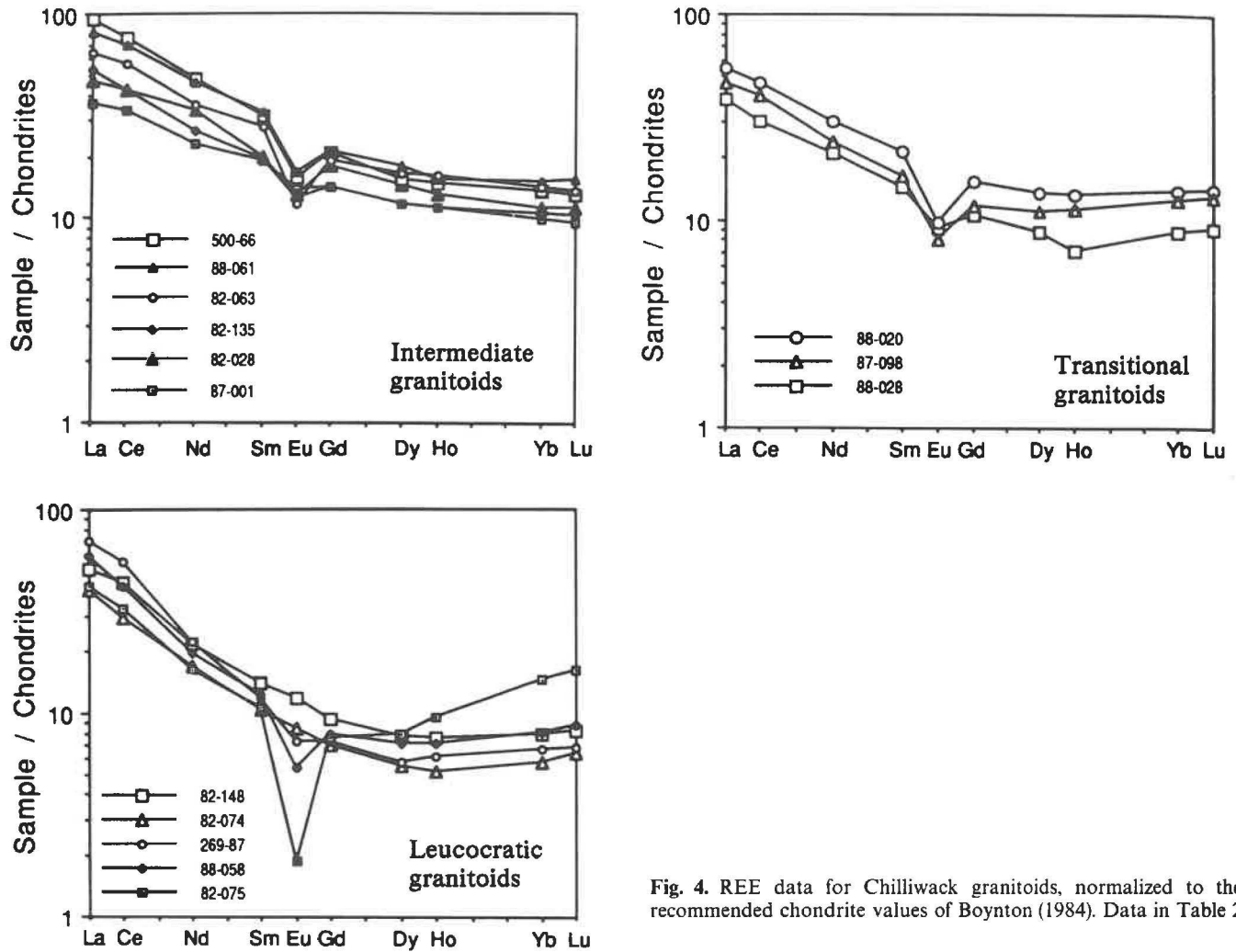
Fig. 4. REE data for Chilliwack granitoids, normalized to the recommended chondrite values of Boynton (1984). Data in Table 2

Table 3. Whole rock isotopic data

Sample No.	Age (Ma)	Rb (ppm)	Sr (ppm)	$^{87}Rb/^{86}Sr$	$^{87}Sr/^{86}Sr$	$^{87}Sr/^{86}Sr_i$	$^{143}Nd/^{144}Nd$	$\varepsilon_{Nd}(0)$
Intermediate Granitoids								
CB82-028	18 ± 17[a]	55.0	301	0.5261	0.704340	0.704205	0.512819	+ 3.59
CB82-135	18 ± 17[a]	45.1	383	0.3393	0.704141	0.704054	0.512862	+ 4.43
CB88-061	2.6 ± 0.3[b]	64.0	403	0.4572	0.703656	0.703643	0.512919	+ 5.54
RWT500-66	10.5 ± 0.9[b]	90.2	362	0.7176	0.703933	0.703826	0.512878	+ 4.74
Transitional granitoids								
CB87-098	18 ± 17[a]	65.5	247	0.7627	0.704324	0.704129	0.512824	+ 3.69
CB88-020	18 ± 17[a]	83.8	233	1.0350	0.704559	0.704294	0.512805	+ 3.32
CB88-028	18 ± 17[a]	46.9	365	0.3695	0.704137	0.704043	0.512847	+ 4.14
Leucocratic granitoids								
CB82-074	8.7 ± 0.3[c]	56.6	279	0.5843	0.704174	0.704102	0.512867	+ 4.53
CB88-058	18 ± 17[a]	71.2	185	1.1066	0.704399	0.704116	0.512868	+ 4.55
RWT269-87	32 ± 2[d]	78.5	277	0.8148	0.703730	0.703360	0.512865	+ 4.49
R-212	30.3 ± 0.1[c]	101.3	34	8.6809	0.707805	0.704069	0.512901	+ 5.19

Analytical uncertainties for Rb and Sr concentrations are 0.1% and 5% respectively. Sr isotope ratios normalized to $^{86}Sr/^{88}Sr = 0.1194$; analytical uncertainty (2σ) is 0.000040 based on 41 analyses of NBS987 with an average measured $^{87}Sr/^{86}Sr = 0.71026$. Nd isotope ratios were normalized to $^{146}Nd/^{144}Nd = 0.7219$ and have 2σ analytical uncertainty = 0.000024, based on 36 analyses of La Jolla Nd with an average measured $^{143}Nd/^{144}Nd = 0.511849$. $\varepsilon_{Nd}(0)$ values were calculated relative to 0.512635. Measured $^{143}Nd/^{144}Nd$ are within analytical error of the initial ratios due to the young age of the Chilliwack plutons. For undated plutons an age of 18 Ma has been assumed. Sources of age data: [a] Undated pluton; [b] Engles et al. (1976); [c] Tepper (1991); [d] R.W. Tabor (written communication, 1992)
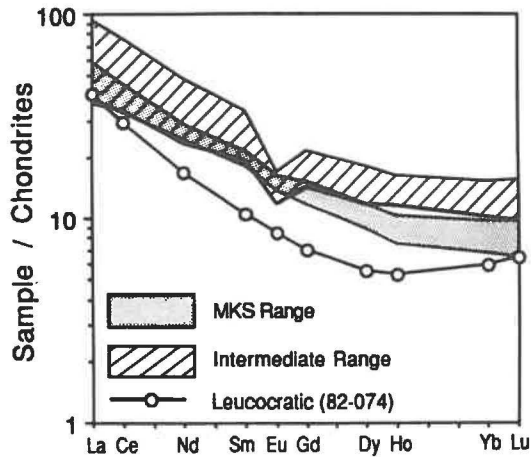
Fig. 5. Comparison of REE patterns of MKS gabbros and their differentiates, *stippled field*, with patterns of intermediate granitoids, *diagonally ruled field*, and leucocratic granitoids. Data for mafic rocks (6 samples) from Tepper (1991); data for granitoids from Table 2

Differentiation of intermediate magmas

A genetic link between the intermediate and leucocratic granitoids is suggested by their close association in space and time, their systematic and near-continuous variation in major and trace element compositions, and their similar initial Sr and Nd isotope ratios. If both types of granitoids differentiated from similar parent magmas, the felsic plutons would presumably represent a greater degree of fractional crystallization. Least-squares mixing calculations indicate that 55–75% crystallization (plagioclase + clinopyroxene + biotite $\pm$ orthopyroxene $\pm$ amphibole) would be required to derive a typical leucocratic granodiorite (82-074 or RWT269-87) from a typical intermediate quartz diorite (87-001 or 82-028). The amounts of crystallization and the proportions of phases removed are relatively insensitive to the mineral compositions used in these calculations (An_{61} or An_{38}, and range of Fe/Mg ratios for mafic silicates). Large degrees of fractionation conflict with the fact that intermediate and leucocratic plutons contain similar levels of incompatible trace elements (Rb, Cs, Th, La) and K_2O. (The leucocratic samples contain more alkali feldspar not because they have higher K_2O, but because they have lower FeO and MgO, and thus less K_2O is contained in biotite). For these elements to maintain constant concentrations during differentiation, biotite or orthoclase removal would be required, along with allanite or monazite (to account for the LREE concentrations). As noted previously, petrographic evidence indicates these minerals formed late and probably were not involved in magma evolution. The lack of systematic K/Rb variation among granitoid samples (281–361) also argues against significant orthoclase or biotite fractionation. A more plausible explanation for similar incompatible trace element contents of the intermediate and leucocratic granitoids is that they originated by similar degrees of melting from sources with similar LILE (large-ion-lithophile-element) contents. The large amounts of feldspar fractionation ($\geq$ 40%) predicted by

the least-squares calculations are also difficult to reconcile with the absence of Eu anomalies in the leucocratic samples. The lack of an anomaly is not attributed readily to co-precipitation of amphibole and feldspar, because least-squares mixing calculations that included amphibole consistently gave worse fits than those that included pyroxene. Furthermore, there is no evidence that the leucocratic magmas were initially vapor saturated, although early saturation would be expected if an intermediate magma that contained enough water to stabilize amphibole (4 wt%; Naney 1983) underwent 50–75% crystallization necessary to produce a leucocratic magma.

In summary, major and trace element data for mafic and granitic plutons indicate: (1) the granitoids cannot be modeled as differentiates of basaltic magmas as represented by coeval gabbros; (2) the leucocratic granitoids cannot be related to the intermediate granitoids by crystal fractionation. The data do not preclude the possibility that some intermediate granitoids were derived by fractional crystallization of basalts not represented by the analyzed mafic rocks. Fractional crystallization might also be responsible for zoning within individual plutons, and/or for contrasts among different plutons of the same group. This would explain, for example, the decrease in $(Eu/Eu^*)_N$ and increase in REE abundances that correlate with increasing SiO_2 in each group. Alternatively, such contrasts may reflect differences in the degree of melting, with lower degree melts having higher SiO_2 and higher REE contents.

It is important to note that samples possibly related by crystal fractionation or differences in degree of melting have similar REE patterns (e.g., 82-028 and 82-063, both from the same pluton). This is because the REE, other than Eu, are not fractionated significantly by removal of the early-formed minerals in these magmas. If relative REE abundances are not affected significantly by fractional crystallization, the implication is that *the REE patterns of the granitoids must reflect the residual mineral assemblages of their source regions*. The negative Eu anomalies in all intermediate plutons point to a source with residual plagioclase, whereas concave upward REE patterns and lack of Eu anomalies in the leucocratic plutons suggest a source containing significant residual amphibole.

Influence of water fugacity on crustal melting

The inferred mineralogical contrasts do not require chemically distinct sources, but instead may arise from differences in f_{H_2O} during melting of an amphibolitic source. Experimental studies have shown that water fugacity strongly influences melt composition and residuum mineralogy during partial melting of basaltic compositions at mid- to lower-crustal pressures (e.g., Holloway and Burnham 1972; Helz 1976; Beard and Lofgren 1989, 1991; Wolf and Wyllie 1989). These experiments may be divided into vapor-saturated experiments, conducted in the presence of an H_2O or $H_2O\text{-}CO_2$ vapor, and dehydration-melting experiments, in which the only water available during melting is that released by breakdown of hydrous silicates. Depending upon bulk composition, dehydration melting of amphibolite yields 6–60% melt at

900–1000 °C; vapor-saturated melting yields similar amounts of melt at slightly lower temperatures, 800–950 °C (Beard and Lofgren 1991; Rushmer 1991; Wolf and Wyllie 1989). However, melt compositions and residual mineral assemblages in the two cases are quite different. Liquids produced by dehydration melting are "tonalitic" and coexist with a residuum dominated by plagioclase, pyroxene, and Fe-Ti oxides (Beard and Lofgren 1991; Rushmer 1991; Wolf and Wyllie 1989). In contrast, melts generated in the presence of an H_2O-rich vapor phase are high in silica and alumina, low in iron and magnesium, and coexist with a residuum of amphibole, clinopyroxene, Fe-Ti oxides and minor plagioclase (Helz 1976; Beard and Lofgren 1991).

These experimental data suggest that the full spectrum of Chilliwack granitoids may be derived from similar amphibolitic sources, with the intermediate plutons originating by dehydration melting and the leucocratic ones by melting under higher f_{H_2O}. This does not require that the leucocratic plutons crystallized from water-saturated magmas because, as recognized by Helz (1976) and others, melt composition in this case is dependent primarily upon P_{H_2O}, rather than P_{TOTAL}. For a given starting material, melts produced at $P_{H_2O} = 3$ kbar will be similar in composition regardless of whether or not the system is vapor saturated (i.e., even if $P_{TOTAL} > 3$ kbar). The main effects of increased f_{H_2O} during melting are to increase the amount of amphibole and decrease the amount of plagioclase in the residuum. These changes in mode are reflected in melt composition, most noticeably in SiO_2, Al_2O_3, MgO, and FeO, and to a lesser extent in CaO; Na_2O and K_2O contents are more dependent upon source composition (Beard and Lofgren 1991).

Beard and Lofgren (1989) noted that liquids produced by dehydration melting of greenstones and amphibolites are similar in composition to arc tonalites, and suggested that this process may be important in the generation of silicic low-K arc magmas. In the case of the Chilliwack, production of intermediate granitoid magmas by dehydration melting is supported by the compositional similarities between the granitoids and the experimental glasses produced by 20–50% melting of greenstones and amphibolites at 950–1000 °C and $P_{H_2O} \leq 1$ kbar (Beard and Lofgren 1991; Rushmer 1991; Wolf and Wyllie 1989)
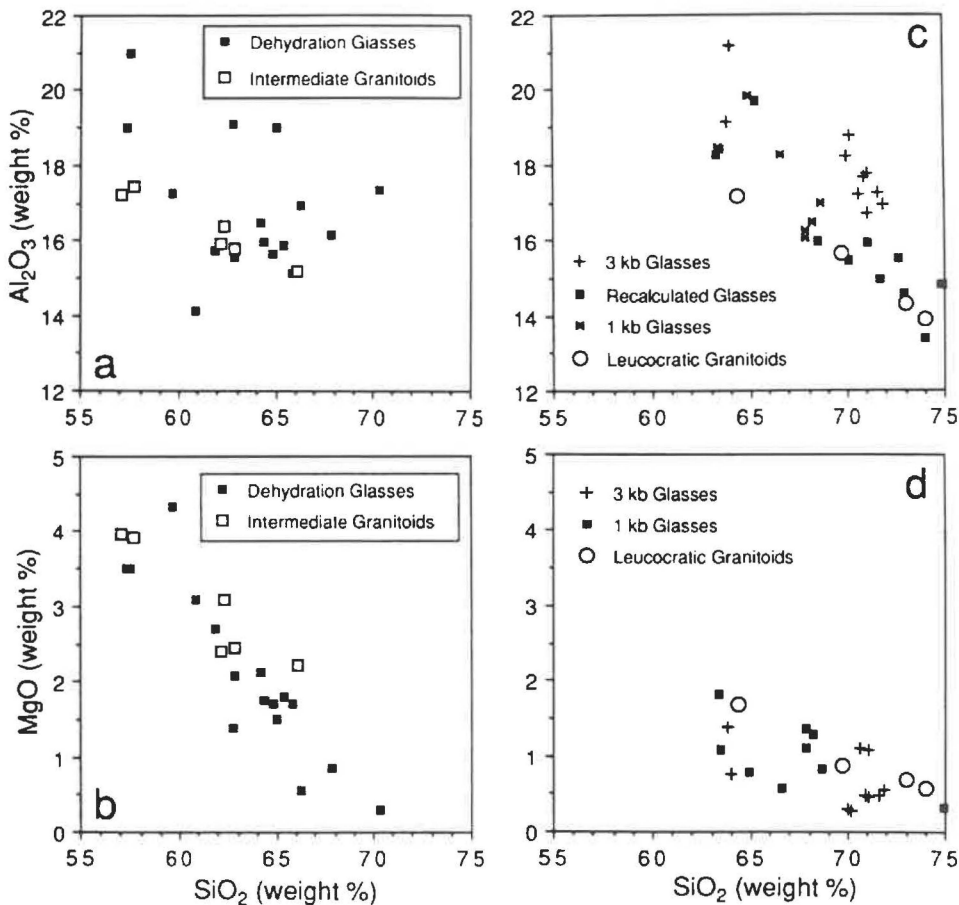

Fig. 6 a–d. Comparison of Chilliwack granitoid compositions with glasses produced by melting of greenstone and amphibolite at different f_{H_2O}. Granitoid data from Table 2; glass analyses from Beard and Lofgren (1991), Rushmer (1991), and Wolf and Wyllie (1989): **a, b** Al_2O_3 and MgO contents of intermediate granitoids compared with those of glasses produced by dehydration melting at 950–1,000°C. **c** Al_2O_3 contents of leucocratic granitoids compared with glasses produced by water-saturated melting at 1 and 3 kbar P_{TOTAL}. Also shown are compositions of 3 kbar glasses recalculated for $P_{TOTAL} = 10$ kbar. Note the overlap between the recalculated glass compositions and the granitoid analyses. **d** MgO contents of leucocratic granitoids compared with those of glasses produced by water-saturated melting at 1 and 3 kbar P_{TOTAL}

(Fig. 6a, b). The granitoids generally have higher K_2O contents than the glasses, but this is probably largely a consequence of differences in source composition. Melting of a source similar in bulk composition to the Chilliwack gabbros (0.2–2.1 wt% K_2O) would produce melts having higher K_2O contents than the experimental glasses, which were produced from starting materials containing 0.03–0.44 wt% K_2O.

Leucocratic Chilliwack granitoids, when compared with intermediate samples at equal SiO_2, are higher in Al_2O_3 and lower in MgO (Fig. 3). Similar trends are observed with increased f_{H_2O} among the experimental glasses (Beard and Lofgren 1991). Generation of the leucocratic granitoids at higher f_{H_2O} is also suggested by their closer resemblance to glasses formed at 1 kbar P_{H_2O} than to those formed by dehydration melting (Beard and Lofgren 1991). However, compositions of the leucocratic granitoids do not resemble those of glasses that coexist with amphibole-rich residua ($P_{H_2O} \geq 3$ kbar) (Fig. 6c). Glasses produced by Beard and Lofgren (1991) during vapor-saturated melting of amphibolite at $P \geq 3$ kbar are strongly peraluminous, high in CaO, very low in FeO and MgO, and do not resemble any naturally occuring rock type. This led Beard and Lofgren (1989) to conclude that vapor-saturated melting at $P \geq 3$ kbar is not a plausible mechanism for the generation of island arc magmas. We suggest, instead, that the leucocratic granitoid magmas formed by vapor-undersaturated melting with $P_{H_2O} \approx 2$ kbar, and that compositional differences between these granitoids and the glasses produced by Beard and Lofgren (1991) at 3 kbar P_{H_2O} result primarily from generation of the Chilliwack magmas at lower P_{H_2O} and higher P_{TOTAL}. Melting at 2 kbar P_{H_2O} instead of 3 kbar P_{H_2O} would lead to higher plagioclase/amphibole in the residuum, which would decrease levels of CaO and Al_2O_3 in the melt, and increase levels of FeO and MgO. Increased P_{TOTAL} would also lower the Al_2O_3 content of the melt because the Al content of amphibole increases with pressure (Hammarstrom and Zen 1986). Thus, although melts formed at $P_{TOTAL} = P_{H_2O} = 3$ kbar are peraluminous, the same may not be true for melts formed at higher P_{TOTAL}. No experimental data are available for melting of amphibolite at 10 kbar with $P_{H_2O} = 3$ kbar, but we have estimated the Al_2O_3 contents of melts formed at these conditions by mass balance, using modal data from the 3 kbar vapor-saturated experiments of Beard and Lofgren (1991). We have assumed the only effect of higher P_{TOTAL} is an increased Al:Si ratio in amphibole and clinopyroxene; any pressure effects on other cation substitutions, phase equilibria, or modal abundances have been ignored. The "high pressure" mineral compositions used in these calculations for amphibole (13 wt% Al_2O_3, 43 wt% SiO_2) and clinopyroxene (5 wt% Al_2O_3 and 51 wt% SiO_2) are those of xenocrysts in Chilliwack gabbros which, based on their Al_2O_3 contents, are interpreted as having come from middle to lower crustal depths (Tepper 1991). The amphibole composition is also similar to those reported from the Round Valley tonalite, which is estimated to have crystallized at a pressure of 8 kbar (Hammarstrom and Zen 1986). Recalculated melt compositions contain higher SiO_2, an average of 3 wt% less Al_2O_3, and are only weakly peraluminous (A/CNK ≤ 1.1). Leucocratic Chilliwack samples overlap in composition with these recalculated glass compositions (Fig. 6c), consistent with the hypothesis that these granitoids originated at higher f_{H_2O} than those of the intermediate group.

Trace element modeling

Results of trace element modeling also support the hypothesis that intermediate and leucocratic granitoids originated by melting of similar sources at different f_{H_2O}. Model calculations assume non-modal batch melting, but because the stoichiometries of the melting reactions are not well known, we have used a modal batch melting equation and varied the mode as a function of melt fraction. The mode of the source as a function of melt fraction and f_{H_2O} was estimated from the data of Beard and Lofgren (1991). Distribution coefficients for andesitic and dacitic bulk compositions (Appendix II) were taken from the literature. The REE abundances of the model source were assumed to lie within a range bracketed at the low end by the least-fractionated Chilliwack gabbro (87-060; Tepper 1991), and at the high end by a calc-alkaline basalt from Crater Lake (no. 1530; Bacon 1990). Gabbro 87-060 [Mg no. = 0.56; $(Eu/Eu^*)_N = 0.84$] does not represent a primary magma, and probably underwent some differentiation during ascent through the crust. For the purposes of source modeling, we have attempted to remove the effects of intracrustal differentiation by adjusting REE abundances of 87-060 for fractional crystallization of 19% plagioclase and 13% olivine. This raises the Mg no. of the sample to 0.79 [equilibrium with Fo_{92} mantle olivine, assuming K_D (ol/liq) (Fe/Mg) = 0.324 (calculated for 10 kbar after Ulmer 1989), and $(Fe^{2+}/(Fe^{3+} + Fe^{2+}))_{magma} = 0.9$], lowers the REE contents, and removes the Eu anomaly, but otherwise does not fractionate the REE. All analyzed MKS samples have REE abundances within the model source range.

The modeled REE patterns closely match those observed for Chilliwack granitoids. Patterns calculated for 35–45% dehydration melting are quite similar to those of the intermediate rocks (Fig. 7a). At $f_{H_2O} = 2$ kbar, 40% melting of the same sources yields melts with concave upward REE patterns similar to those of leucocratic plutons (Fig. 7b). The pronounced difference in REE patterns, at comparable degrees of melting, reflects the strong influence of f_{H_2O} on the stability of amphibole during melting. During dehydration melting, amphibole is consumed and the model residuum consists of 50% plagioclase, 27% clinopyroxene, 14% orthopyroxene, and 9% Fe-Ti oxides. At higher f_{H_2O}, amphibole remains an important phase in the residuum (25%), accompanied by 40% plagioclase, 20% clinopyroxene and 15% Fe-Ti oxides. Calculated abundances of Rb, Sr, Cr, Sc and Ni are also consistent with the model, although the uncertainties in source concentrations and distribution coefficients (particularly for transition metals) are larger for these elements than for the REE. However, the lower Sr contents of the leucocratic samples do require that feldspar be a major constituent of the residuum for these as well as the intermediate plutons. Higher Ba concentrations in the
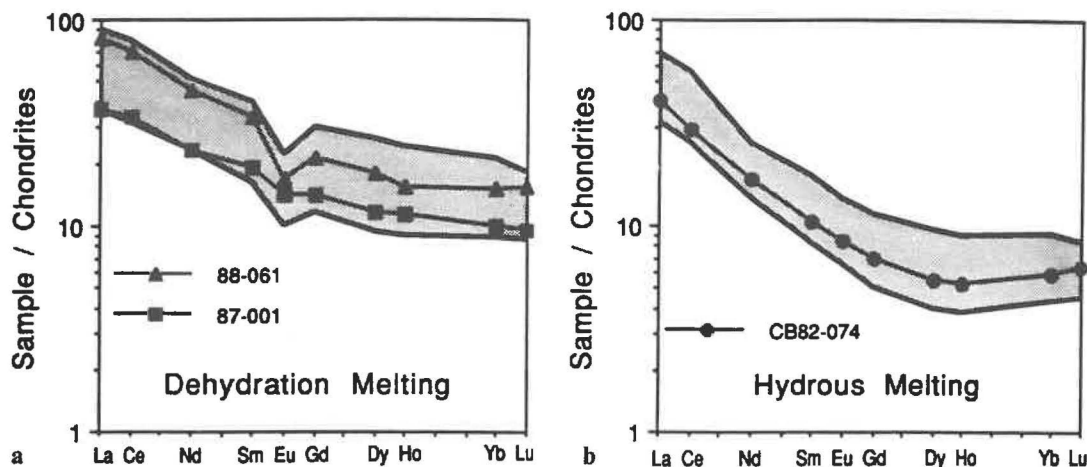
Fig. 7a, b. Calculate REE patterns, *stippled fields*, compared to those of representative intermediate and leucocratic granitoids: **a** Patterns calculated for 35–45% dehydration melting, leaving a residuum consisting of 50% plagioclase, 27% clinopyroxene, 14% orthopyroxene, and 9% Fe-Ti oxide. Data for intermediate grani- toids 87-001 and 88-061 are shown for comparison. **b** Patterns calculated for 35–40% melting of same sources, but at 2 kbar P_{H_2O}, leaving a residuum of 40% plagioclase, 25% amphibole, 20% clinopyroxene, and 15% Fe-Ti oxides. Data for leucocratic granitoid 82-074 are shown for comparison

leucocratic samples readily are not attributed to differ- ences in residuum mineral assemblage or degree of mel- ting, and may reflect trace element heterogeneity of the source.

Sr and Nd isotope compositions

Measured Sr and Nd isotope compositions of 10 mafic samples (Tepper 1991) and 11 granitoid samples (Table 3) demonstrate that: (1) initial isotope compositions of gabb- ros and granitoids overlap; (2) all granitoids from inter- mediate through leucocratic have similar initial ratios (Fig. 8). These observations are consistent with derivation of the granitoids from a source represented by the exposed gabbros. Chilliwack samples show an inverse correlation between initial $^{87}Sr/^{86}Sr$ and $^{143}Nd/^{144}Nd$, which is probably mostly a result of high-level assimilation-frac- tionation processes (AFC). Isotopic variation among MKS gabbros and diorites from Mt. Sefrit ($^{87}Sr/^{86}Sr_i$ $= 0.7034$–0.7040; $\varepsilon_{Nd}(0) = +4.8$ to $+3.5$) can be mo- deled by about 10% wallrock assimilation during shal- low-level AFC (Tepper 1991), and a similar process could account for isotopic variability among the granitoids. AFC is consistent with the observation that all granitoids with $\varepsilon_{Nd} < +3.7$ (82-028, 87-098, and 88-020) have large negative Eu anomalies. Conversely, leucocratic samples with $(Eu/Eu^*)_N$ close to one (RWT269-87, 82-074) have $\varepsilon_{Nd} > +4.4$, consistent with the interpretation that they have undergone limited crystal fractionation and thus less assimilation. These plutons still could be contaminated, of course, either by AFC during *in situ* crystallization after emplacement, or by incorporation of xenoliths (which need not be accompanied by crystallization). Compared to the mafic rocks, the granitoids have slightly higher average $^{87}SR/^{86}Sr_i$ (0.7040 vs 0.7038) and slightly lower average $\varepsilon_{Nd}(0)$ values ($+4.4$ vs $+5.0$). This may reflect greater sensitivity of the granitoids to crustal contamina- tion because of their lower concentrations of Sr and, in some samples, Nd.
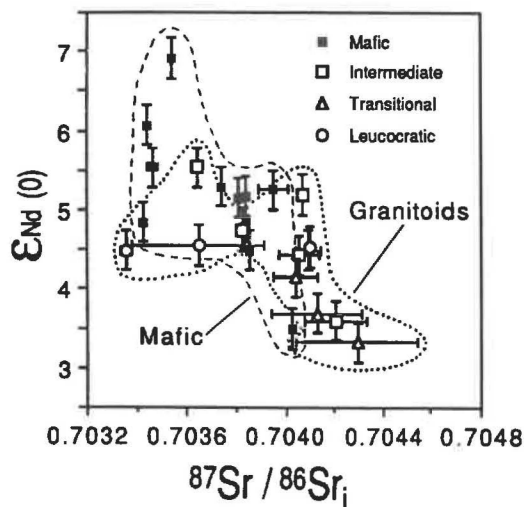

Fig. 8. Initial Sr isotopic composition and ε_{Nd} (0) of 22 mafic and granitoid samples from the Chilliwack batholith. Samples with large uncertainties in $^{87}Sr/^{86}Sr_i$ are from undated plutons, and have initial ratios calculated for an age of 18 ± 17 Ma. Note the significant overlap between ratios of mafic samples, *dashed field*, and granitoid samples, *dotted field*, and the lack of systematic differences in ratios among the three granitoid groups. Data for mafic samples from Tepper (1991); granitoid data in Table 3

Pressure, temperature, and f_{H_2O} during melting

At pressures of 10–15 kbar tonalitic liquids coexist with garnet under both vapor-saturated and vapor-absent conditions (Huang and Wyllie 1986; Rutter and Wyllie 1988; Wolf and Wyllie 1989; Carroll and Wyllie 1990). None of the Chilliwack granitoids shows the HREE depletion predicted for melts that equilibrated with re- sidual garnet, which suggests they formed at lower pres- sures. However, the high temperatures required for am- phibolite melting (see heat transfer calculations) restrict this process to the deep crust (probably not more than

10 km above the crust-mantle boundary, which has a present-day depth of 40 km (Mooney and Weaver 1989). Assuming a crustal density of 2.7 gm/cm³, this corresponds to a pressure of 8–10 kbar. The depth to the crust-mantle boundary may have varied during the course of Cascade magmatism, but probably has not changed significantly since 2.6 Ma, the age of the youngest dated pluton in the batholith (Engels et al 1976).

Temperatures in the lower crust *during* generation of the leucocratic granitoid magmas cannot have exceeded 1,070 °C, the thermal stability limit of amphibole in basalt at 10–15 kbar (Allen and Boettcher 1978). This is an upper limit because the thermal stability of amphibole is lower in more silica-rich melts (Allen and Boettcher 1978; Holloway and Burnham 1972). Data from the melting experiments of Beard and Lofgren (1991) also support production of the intermediate magmas at 950–1000 °C, and the leucocratic magmas at 850–950 °C. The temperature at which a melt separated from its source may be estimated from its P_2O_5 content, using the apatite solubility expression of Harrison and Watson (1984):

$$\ln D = [(8,400 + ((SiO_2\text{-}0.5)\,2.64 \times 10^4))/T]\text{-}[3.1 + 12.4\,(SiO_2\text{-}0.5)]$$

in which D is the apatite/melt distribution coefficient for P, SiO_2 is the weight fraction silica in the melt, and T is in kelvins. This approach assumes the melt formed in equilibrium with residual apatite and has not undergone subsequent chemical modification by crystal fractionation, assimilation, etc. The first requirement may be satisfied during melting of mafic crust (Beard and Lofgren 1989), particularly at lower degrees of melting. The second requirement is difficult to evaluate, but among Chilliwack samples is most likely to be a valid assumption for the leucocratic samples in which, as noted above, the lack of a Eu anomaly argues against significant crystal fractionation. Temperatures calculated for these samples (which vary in P_2O_5 content by a factor of three and in SiO_2 content by almost 10 wt%) cluster between 880–900 °C, in good agreement with temperature estimates based on phase equilibria. In contrast, temperatures calculated for the intermediate and transitional granitoids are quite variable (807–917 °C), and are below those inferred from comparison with experimental glasses. The more-mafic quartz diorites also yield the lowest temperatures, suggesting either that these magmas were not in equilibrium with apatite at the time of separation, or that they have undergone subsequent differentiation.

Based on the late crystallization of amphibole, the intermediate granitoids in the Chilliwack probably crystallized from magmas that initially contained ≤ 2 wt% H_2O (based on a petrographic estimate that 50% crystallization of anhydrous phases occurred prior to amphibole saturation, and assuming 4 wt% H_2O is required to stabilize amphibole (Naney 1983)). Low water contents for intermediate plutons also are indicated by the scarcity of aplites and miarolitic cavities. For the leucocrtic plutons, several lines of evidence suggest crystallization from magmas with higher water contents:

1. They contain a greater abundance of aplite and pegmatite dikes.

2. Amphibole in these rocks, where present, lacks pyroxene cores and appears early-formed, indicating the melt contained ≥ 4 wt% H_2O (Naney 1983). For leucocratic samples that contain no amphibole (e.g., 88-058) the only petrographic constraint on water content comes from the crystallization of biotite before alkali feldspar, which indicates a minimum water content of 2.5 wt% (Wyllie et al. 1976).

3. Amphiboles in the leucocratic granitoids have higher Mg-number than those in the intermediate plutons, although whole rock Mg-numbers for the leucocratic samples are lower. A correlation between f_{H_2O} and the Mg-number of ferromagnesian minerals has been observed in other batholiths, higher f_{H_2O} being associated with higher Fe^{3+}/Fe^{2+} and, in turn, higher $Mg/(Mg + Fe^{2+})$ ratios (Czamanske and Wones 1973; Dilles 1987).

4. Apatite from leucocratic Chilliwack plutons has molecular Cl/F $\leq$ 0.05, distinctly lower than ratios in apatite from intermediate plutons (Cl/F = 0.23–0.47) (Tepper 1991). Apatite with a low Cl/F ratio may indicate crystallization from a vapor-saturated magma, because in a vapor-saturated magma Cl partitions strongly into the vapor phase (Kilinc and Burnham 1972) whereas F partitions into the melt (Burnham 1979a). Vapor saturation of a granitic magma at 2 kbar would require about 6.5 wt% H_2O (Wyllie et al. 1976). However, because the apatite analyzed in the leucocratic sample is small and interstitial, it is not possible to establish how much crystallization took place before the melt became saturated, so 6.5% represents an upper limit for the water content.

5. The REE patterns of the leucocratic granitoids require significant amphibole in the residuum after melting, which implies $P_{H_2O} > 1$ kbar (Beard and Lofgren 1991). The water content of a melt formed at 2–3 kbar P_{H_2O} and 10 kbar P_{TOTAL}, calculated after Burnham (1979b), is 3.2–4.3 wt%. This range is below that determined by Beard and Lofgren (1991) for glasses produced at 3 kbar P_{H_2O} (5.3–11.6 wt%). However, their estimates are based on summation differences and represent maximum values because of Na loss and calculation of all Fe as FeO. In summary, the mineralogical and geochemical evidence suggest the Chilliwack granitoid melts that formed in equilibrium with residual amphibole probably contained on the order of 4 ± 1 wt% H_2O.

The source of the water

Crystallization of mantle-derived basaltic magmas near the base of the crust can provide heat required to drive melting, and can add hydrous fluids to the lower crust. Variations in the water contents of these basalts, and hence variations in the amount of water exsolved as they crystallize, could account for the inferred differences in f_{H_2O} during generation of Chilliwack granitoids. The LKS and MKS gabbros document the existence of relatively anhydrous basalts (< 1 wt% H_2O) during Chilliwack plutonism. Evidence of basalts with higher water contents is provided by tschermakitic amphibole xenocrysts (Table 2) that are present in some MKS gabbros. These xenocrysts are similar in composition to amphiboles in lower crustal xenoliths from the Aleutians (Conrad and Kay 1984), Lesser Antilles (Arculus and Wills 1980), and Japan

(Takahashi 1986) that have been interpreted as early-formed crystals from primitive hydrous basalts. In these arcs crystallization of amphibole at upper mantle or lower crustal depths from basalt that has undergone little prior fractionation implies that the water was acquired from the mantle rather than by interaction with crustal rocks. The basaltic magma from which the Chilliwack amphibole xenocrysts formed is calculated (using distribution coefficients from Irving and Frey 1984) to have had a flat REE pattern with concentrations about 10 times chondritic, 300–500 ppm Sr, 100–300 ppm Ni, and no Eu anomaly. These characteristics suggest a hydrous basalt that had not undergone significant feldspar fractionation.

The water content necessary for early crystallization of amphibole from a basaltic melt ($\geq$ 3 wt%; Eggler 1972) is greater than the water content of the resulting rock (approximately 1 wt%, assuming 50% amphibole). Thus a basalt that contains sufficient water to crystallize amphibole will, at some point during solidification, exsolve a hydrous fluid. In the scenario envisioned for the Chilliwack, basaltic magmas with a range of water contents are emplaced into amphibolitic lower crust that is at or even slightly above its solidus. Emplacement of a basalt with a low water content (e.g., LKS or MKS magmas) would lead to melting at low f_{H_2O} (dehydration melting) because little water would be exsolved during crystallization. The melt would be intermediate in composition, leaving behind an amphibole-poor residuum. Conversely, emplacement of a hydrous basalt would result in melting at higher f_{H_2O}, because more water would be exsolved during solidification. This water would dissolve in the newly formed granitic melt, raising its f_{H_2O} (but not to the point of saturation). These conditions would enhance amphibole stability in the residuum, and favor production of a siliceous melt. Mass balance estimates suggest the volume of water exsolved during crystallization of a basalt with 3 wt% H_2O would be sufficient to stabilize an amphibole-rich residuum during granitoid melt generation if the ratio of melt generated/basalt crystallized is 0.3–0.6 (as predicted from heat transfer calculations, see below).

Heat transfer calculations

The model developed above on the basis of chemical and isotopic data requires efficient, large-scale transfer of heat from mafic magmas to the lower crust. To evaluate whether underplating can provide sufficient heat to generate pluton-scale volumes of granitoid magma (> 100 km³) from amphibolite, we have performed a series of one-dimensional conductive heat transfer calculations designed to investigate the following questions: (1) what initial wallrock temperatures are necessary for amphibolite to yield large volumes of granitoid magma; (2) what is the efficiency of melt production (ratio of melt produced/basalt crystallized) as a function of initial wallrock temperature; (3) what are the time and length scales associated with melt production from amphibolite by underplating?

The calculations are based on an underplating model in which basaltic magma at its liquidus temperature (T_L) is emplaced instantaneously into country rock having a uniform initial temperature (T_{CR}). In response to conductive heat loss, the basalt cools and begins to crystallize, forming a zone of crystal-liquid mush at the contact. Simultaneously, the influx of heat into the wallrock may result in partial melting and development of a mush zone in the country rock at the contact. These crystallization and melting reactions are coupled, and their progress is dependent upon the rate of heat transfer from the basalt to the wallrock. The rate of heat transfer, in turn, is a function of the temperature gradient across the contact and the variation in solid fraction in both the basalt and the wallrock over the temperature range of interest.

Modeling of melt generation driven by underplating requires solving the coupled heat transfer equations for both the basalt and the wallrock. These equations have been solved using the method of Berganntz (1989), in which both country rock and basalt are subdivided into a series of subdomains bounded by isotherms. Isotherms are chosen such that temperature and melt fraction vary linearly within each subdomain. Temperature as a function of time within each subdomain is given by:

$$\partial T_i/\partial t = \kappa_i \, \partial^2 T_i/\partial x_i^2 + (L_i/Cp_i)\,(dfs_i/dt)$$

where x_i and t are the independent variables distance and time, T_i is temperature, κ_i is thermal diffusivity, L_i is specific latent heat, Cp_i is specific heat capacity, and fs_i is solid fraction, all in the ith subdomain. In these calculations we assumed the basalt had $T_L = 1,200\,°C$ and $T_{SOLIDUS} = 1,005\,°C$. The country rock solidus was taken to be 800 °C, and T_{CR} was investigated at 600, 700, 800 and 850 °C. Except at 850 °C, where there were numerical instabilities in the program, two sets of calculations were performed for each T_{CR}, one for dehydration melting and one for melting with $f_{H_2O} = 3$ kbar. Solid fraction as a function of temperature was estimated for both types of melting from the data of Beard and Lofgren (1991), Clemens and Vielzeuf (1987), Helz (1976), and Holloway and Burnham (1972). Other thermochemical parameters (assumed constant) used in these calculations are: heat capacity: 1,200 J/kg-K; enthalpy of fusion: 3.5×10^5 J/kg; thermal conductivity: 3.62×10^7 J/m-K-year; and bulk density: 2.6×10^3 kg/m³.

The results of these calculations are summarized in terms of temperature profiles across the contact (isotherm positions) at selected time intervals after intrusion (Table 4). For a given T_{CR} and time interval, the profiles for dehydration and hydrous melting are nearly identical. However, more melt is produced with $f_{H_2O} = 3$ kbar because higher f_{H_2O} results in more melting at the same temperature. The total thickness of melt generated in each case was calculated by assuming that melt fraction (F_L) varied linearly within each subdomain, and then summing the four wallrock subdomains. The same approach was used to calculate the total thickness of basalt crystallized (B_{XL}) within the intrusion. The variable that most strongly influences melt production is T_{CR}. At high T_{CR}, not only is the wallrock closer to its solidus, but also the thermal gradient across the contact is shallower, meaning that the rate of heat diffusion *within the intrusion* (from the interior into the layer against the contact) is closer to the rate of heat diffusion *out of the intrusion* into the wallrock. Under these conditions, heat transferred to the crust results from

Table 4. Isotherm positions at selected time intervals after intrusion

Isotherm °C	Dehydration melting; T_{CR} = 800 °C				Isotherm °C	Dehydration melting; T_{CR} = 600 °C			
	50 kyear	200 kyear	500 kyear	900 kyear		50 kyear	200 kyear	500 kyear	900 kyear
1,200°	− 1,317	− 2,638	− 4,174	− 5,602	1,200°	− 1,369	− 2,744	− 4,342	− 5,828
1,175°	− 873	− 1,749	− 2,767	− 3,713	1,175°	− 955	− 1,913	− 3,026	− 4,062
1100°	− 387	− 776	− 1,227	− 1,647	1100°	− 513	− 1,028	− 1,627	− 2,184
1050°	− 156	− 313	− 496	− 666	1050°	− 342	− 626	− 990	− 1,329
1,013° (cont)	0	0	0	0	962° (cont)	0	0	0	0
900°	608	1,215	1,920	2,575	900°	224	445	703	943
850°	1,057	2,112	3,339	4,479	800°	629	1,256	1,985	2,662
815°	1,680	3,358	5,309	7,123	620°	2,012	4,023	6,360	8,533
800°	2,811	5,620	8,886	11,921	600°	3,005	6,009	9.500	12,745

Isotherm	Melting at 3 kbar P_{H_2O}; T_{CR} = 800 °C				Isotherm	Melting at 3 kbar P_{H_2O}; T_{CR} = 600 °C			
	50 kyear	200 kyear	500 kyear	900 kyear		50 kyear	200 kyear	500 kyear	900 kyear
1,200°	− 1,325	− 2,654	− 4,199	− 5,635	1,200°	− 1,374	− 2,754	− 4,358	− 5,849
1,175°	− 885	− 1,773	− 2,806	− 3,765	1,175°	− 962	− 1,928	− 3,050	− 4,094
1100°	− 406	− 814	− 1,288	− 1,729	1100°	− 524	− 1,051	− 1,623	− 2,231
1050°	− 180	− 362	− 572	− 769	1050°	− 325	− 653	− 1,033	− 1,387
1,006° (cont)	0	0	0	0	957° (cont)	0	0	0	0
900°	546	1,090	1,723	2,310	900°	202	402	635	851
850°	,964	1,926	3,044	4,084	800°	607	1,212	1,915	2,568
815°	1,562	3,122	4,936	6,622	620°	2,005	4,008	6,336	8,501
800°	2,750	5,499	8,694	11,663	600°	3,000	5,999	9,485	12,725

Isotherm positions (in meters) are given relative to the contact, cont, which remains at fixed temperature and location. Negative distances indicate positions within the intrusion; positive distances are within the wallrock. Note that wallrock isotherms reported for T_{CR} = 800 °C are different from those reported for T_{CR} = 600 °C. Important points are: (1) For a given T_{CR} and time after intrusion, isotherm positions for dehydration and 3kbar P_{H_2O} melting are very similar; (2) distance over which wallrock is heated above 800 °C is over four times greater with T_{CR} = 800 °C than with T_{CR} = 600 °C

a smaller amount of cooling of a thicker layer of the intrusion rather than from a larger amount of cooling of a thinner layer at the contact. Thus, after 500,000 years the thickness of the solidified basalt layer at the contact is 496 m with T_{CR} = 800 °C versus 990 m with T_{CR} = 600 °C, even though the total amount of basalt crystallized, which includes contributions from the partially solidified subdomains inside the intrusion, is comparable in both cases (2,104 m vs 2,435 m). With the thinner marginal zone of solid basalt at higher T_{CR}, the rate of heat transfer into the wallrock is increased. The net result of faster heat transfer and higher T_{CR} is that after 500,000 years the distance over which the wallrock has been heated above its solidus is over four times greater for T_{CR} = 800 °C than it is for T_{CR} = 600 °C (Table 4).

To estimate the amount of melt that is extractable (M_{EX}), we have applied the melt segregation model of Fountain et al. (1989), which is equivalent to assuming that melt may be extracted only from regions in which F_L > 0.25. Calculated this way, M_{EX} is 10–60% of the total melt generated, and this increases with T_{CR}. The ratio M_{EX}/B_{XL} is a measure of the efficiency of melt production by underplating. For purely conductive heat transfer, this ratio is constant over time, but increases with T_{CR} (Fig. 9). With T_{CR} < 700 °C, M_{EX}/B_{XL} for dehydration melting is < 0.1, implying that over 50 km of underplating would be required to generate a batholith 5 km thick. However, with T_{CR} = 850 °C, (M_{EX}/B_{XL} = 0.24) the required thickness of basalt is reduced to 15–20 km, which is compatible with geophysical data from the Cascades (Mooney and Weaver 1989) that indicate the presence of mafic rock at 10–40 km depth. Based on these calculations, and assum-
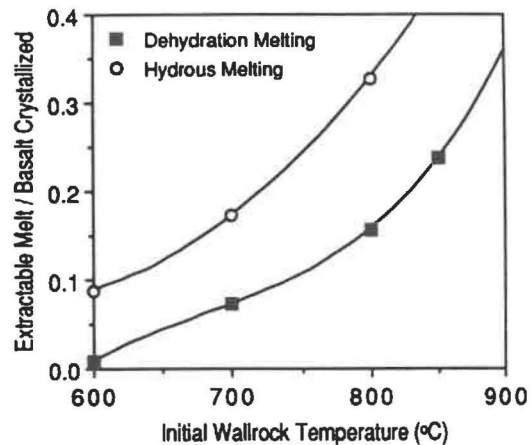
Fig. 9. Plot of the efficiency of melt production (thickness ratio of extractable melt formed to basalt crystallized) as a function of initial wallrock temperature. For conductive heating this ratio remains constant over time

ing dehydration melting with T_{CR} = 850 °C, a typical intermediate pluton, with an estimated volume of 150 km³, could be generated in 200,000 years in response to crystallization of 1.3 km of basalt beneath a source region 25 km in diameter.

Summary and discussion of model

Based on trace element and radiogenic isotope data from mafic and granitoid plutons, and the results of conductive

heat transfer calculations, a model has been developed for the generation of Chilliwack granitoids ranging from quartz diorites through leucogranites. In this model (Fig. 10) the granitoid magmas were produced by partial melting of amphibole-bearing mafic lower crust that formed by underplating of basaltic magmas similar in composition to the exposed gabbros. Melting of this lower crust, already close to or slightly above its solidus, was driven by intrusion of mantle-derived basaltic magmas. The process would be most efficient immediately following the underplating event(s) because ambient temperatures $\geq 800\,°C$ are required for large-scale melting by this mechanism. This may explain why basaltic magmatism appears to have been a precursor to granitoid formation in many I-type batholiths (Pitcher 1987). Our model suggests that in the Chilliwack batholith variations in the water contents of these basalts exerted a strong influence on the resulting granitoid melt compositions. Intrusion of relatively anhydrous basalts (represented by LKS and MKS gabbros) resulted in dehydration melting of the lower crust and production of intermediate magmas (quartz diorites and tonalites). The residuum from low-f_{H_2O} melting is plagioclase-rich, as reflected in the negative Eu anomalies of all intermediate plutons. In contrast, intrusion of hydrous basalts (represented in some Chilliwack gabbros by tschermakitic amphibole xenocrysts) resulted in production of leucocratic granodiorites and granites with distinctive concave upward REE patterns and slight or no Eu anomalies. The REE patterns of these plutons reflect a significant proportion of amphibole in the residuum. Plutons with mineralogical and geochemical characteristics transitional between those of the quartz diorites and the leuco-granodiorites may have formed by intrusion of basalts with intermediate water contents. Ultimately these

variations in the water contents of mantle-derived basalts may reflect variability in the amount of water given off by the subducted slab.

This model outlines a chemical as well as physical role for arc basalts in the production of I-type granitoids, and implies that thick crust is a requirement for large-scale generation of arc granitoids. The crust acts as a barrier to basaltic magmas ascending from the mantle wedge, causing them to pond and crystallize, and leading to development of a zone of lower crustal melt generation. Only during the early stages of magmatism, before development of the lower crustal melt zones, are small batches of mafic magma able to ascend to shallow crustal levels, forming the observed gabbros. This model shares some features of previous hypotheses of continental arc magmatism (e.g., Hildreth and Moorbath 1988), but differs in proposing that: (1) fluids exsolved during crystallization of hydrous basaltic magmas may play an important role in controlling crustal melting reactions; (2) variation in f_{H_2O} may exert strong influence on melt compositions; (3) exposed mafic rocks may have crystallized from basalts similar in composition to those that formed the lower crustal granitoid source.

This model attributes much of the lithologic diversity among Chilliwack granitoids to differences in melting reactions. Individual plutons are viewed as discrete batches of magma that underwent limited chemical modification during ascent and emplacement. The model does not preclude the possibility that crystal fractionation, assimilation, and/or mixing may have modified individual magma batches, but we suggest that such processes are of secondary importance in determining the general lithology of a pluton. Thus, crystal fractionation may produce zoning from quartz diorite to granodiorite within an
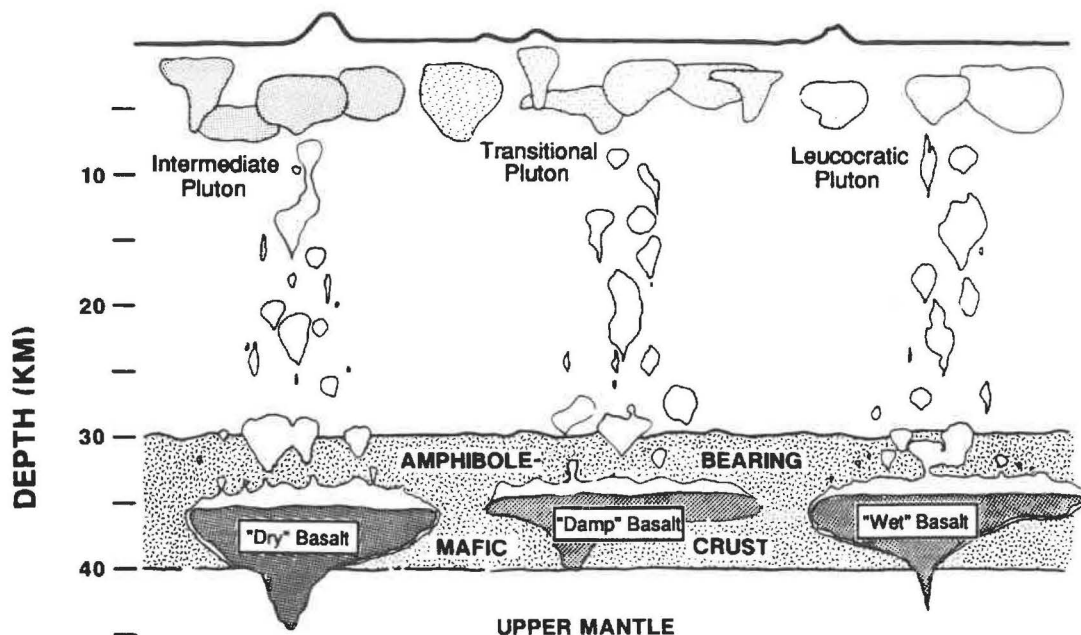

Fig. 10. Cartoon of model for generation of Chilliwack granitoids by melting of amphibolitic lower crust with variable f_{H_2O}. Intrusion/underplating of relatively dry basalts results in dehydration melting and production of intermediate magmas, whereas intrusion of more-hydrous basalts leads to melting at higher f_{H_2O} and formation of more siliceous melts.

individual stock, but this does not change the overall intermediate character of the pluton, which is a function of its derivation by melting of mafic crust at low f_{H_2O}.

Magma mixing may also have modified individual magma batches. For example, mixing of intermediate and leucocratic magmas could account for the transitional granitoids, or there may have been some mixing between the underplating basalts and the granitoid melts. However, the range of granitoid compositions within the batholith cannot be ascribed to mixing of LKS or MKS basalts and leucocratic magmas in different proportions. Aside from scattered mafic inclusions in some intermediate plutons, little field evidence was found for mixing, suggesting that any mixing that took place must have been very efficient, probably occurring at depth between liquids that were not widely different in composition.

Restite unmixing (Chappell et al. 1987) is unlikely to have contributed significantly to petrologic diversity among Chilliwack granitoids. Most intermediate granitoids do contain calcic plagioclase cores, which could be restitic. However, separation of these plagioclases would produce a felsic magma with a lower $(Eu/Eu^*)_N$. Among Chilliwack granitoids the opposite is observed: leucocratic plutons have *higher* $(Eu/Eu^*)_N$ than the intermediate stocks.

The granitoids examined in this study are chemically and mineralogically similar to I-type granitoids in other Cordilleran batholiths, suggesting that this model for the Chilliwack may have wider application. The most distinctive fingerprints of this model are the leucocratic granodiorites or granites with concave upward REE patterns and no Eu anomalies. Rocks with these REE traits, as discussed above, point to melting at elevated f_{H_2O} and are unlikely to result from crystal fractionation. Leucocratic granodiorites with concave upward REE patterns have been described from a number of other Cordilleran batholiths including the Sierra Nevada (Dodge et al. 1982), the Peninsular Ranges (Gromet and Silver 1987), the Coastal batholith of Peru (Boily et al. 1989), and the Sierra Madre Occidental of Mexico (Bagby et al. 1981). In the Peninsular Ranges and in Mexico the leucocratic rocks are associated with quartz diorite and tonalite plutons that have REE patterns similar to intermediate Chilliwack granitoids, suggesting melting of mafic crust with variable f_{H_2O} may have been important in the generation of these batholiths as well.

Appendix I

Analytical methods
Major and trace element analyses. Whole rock major and trace element abundances were determined by inductively coupled plasma emission spectrometry (ICP-ES) on a Baird PS-1 48-channel spectrometer at the University of Washington. Samples were oven-dried at 110 °C for at least 24 hours prior to weighing. Major elements were determined on 0.1 g of rock powder that was fused with lithium metaborate at 1,050 °C and then dissolved in dilute nitric acid containing an internal standard. The spectrometer was calibrated with synthetic and natural standards, and samples were run with a range of natural standards including BHVO-1, ARHCO-1, AGV-1, and GSP-1. Analytical uncertainty, based on analysis of four standards covering the compositional range of the Chilliwack samples, is within 1% for Si and Al, about 2% for Fe, Mg, Ca, and 3–5% for Na (K was run as a trace element). Relative precision for Ti is estimated at 1–2%. Loss-on-ignition was determined by weighing 1 g of sample before and after firing at 1,050 °C for 1 hour. Ferrous iron was determined volumetrically on some samples by titration with ferrous ammonium sulphate.

For determination of trace elements (K, Mn, P, Ni, Cr, Sc, V, Sr, Ba, Zn, Cu, Zr, Be, Li) rock powders (0.5–2.0 depending upon SiO_2 content) were digested in an HF-HNO_3-$HClO_4$ mixture, evaporated, reevaporated with more $HClO_4$ to remove any remaining free F^-, and then dissolved in dilute HCl. Solutions that contained insoluble residues or precipitates were filtered, and the solid material was fused with NaOH, dissolved in dilute HCl, and then combined with the original filtrate. A multielement standard addition was made to an aliquot of this solution, and both solutions were analyzed successively along with standards. The relative precision for this technique is within 5% for most elements except Li (10–15%). In addition, Zr values may be low because of incomplete zircon dissolution.

Rare earth elements were determined by ICP-ES following a mixed HCl-HNO_3 cation exchange technique modified after Crock et al. (1986). The procedure for sample digestion and dissolution was the same as that for other trace elements. Relative precision for REE is 2–5%, and all samples were normalized to RGM-1 or ARHCO-1 which were analyzed during each run as standards.

In addition to the elements determined by ICP-ES, Rb was determined by isotope dilution on a VG Sector mass spectrometer at the University of Washington; Nb, Pb and Ga were determined by XRF on 82-074 and R-212 at the University of Massachusetts at Amherst (J. Sparks, analyst); U, Th, Cs, Hf, Ta, and Sb were determined by INAA on 82-135, 88-028, 82-074, 87-027 amphibole, and 82-074 feldspar at JSC/NASA (D. Mittlefehldt, analyst), and Cs was determined by ICP-MS on 87-001, 87-098, and 88-058 at Union College.

Isotopic analyses. Isotopic analyses for Sr and Nd were performed at the University of Washington using a VG Sector mass spectrometer. Samples (approximately 200 mg) were digested in an HF-$HClO_4$ mixture and redissolved in HCl. Rubidium, Sr, and REE were separated on cation exchange columns; Sm and Nd were separated by means of a second exchange column using 2N methylactic acid, and prior to loading, were cleaned with a third column containing AG-50W X8 resin. Elemental abundances of Sr were measured by isotope dilution only for those samples (mostly mineral separates) for which ICP data were not available. For isotopic analysis approximately 500 ng of Sr was run on a single Ta filament, and the isotopic values were normalized to $^{86}Sr/^{88}Sr = 0.1194$; Nd was analyzed by loading 500 ng and Nd onto the side filament of a Re triple filament and then run as Nd^+.

Appendix II

Distribution coefficients used in REE modeling

	Intermediate compositions				Leucocratic compositions			
Element	Plagioclase	Clinopyroxene	Orthopyroxene	Magnetite	Plagioclase	Clinopyroxene	Amphibole	Magnetite
La	0.130	0.120	0.016	0.010	0.320	0.160	0.600	0.010
Ce	0.090	0.180	0.019	0.010	0.280	0.210	0.900	0.010
Nd	0.063	0.400	0.030	0.010	0.220	0.450	2.800	0.010
Sm	0.045	0.700	0.042	0.010	0.160	0.800	4.000	0.010
Eu	0.920	0.690	0.052	0.010	0.950	0.850	3.450	0.010
Gd	0.037	0.880	0.066	0.010	0.120	1.100	5.500	0.010
Dy	0.029	1.100	0.120	0.010	0.090	1.450	6.200	0.010
Ho	0.026	1.100	0.160	0.010	0.080	1.400	6.100	0.010
Yb	0.023	0.900	0.360	0.010	0.060	1.100	4.950	0.010
Lu	0.022	0.850	0.450	0.010	0.055	1.000	4.500	0.010

Sources: Fujimaki et al. (1984); Green and Pearson (1985); Arth (1976); Arth and Barker (1976)

References

Allen JC, Boettcher AL (1978) Amphiboles in andesite and basalt, II: stability as a function of P-T-f_{H_2O}-f_{O_2}. Am Mineral 63:1074–1087

Arculus RJ, Wills KJA (1980) The petrology of plutonic blocks and inclusions from the Lesser Antilles Island Arc. J Petrol 21:743–799

Arth JG (1976) Behavior of trace elements during magmatic processes–a summary of theoretical models and their applications. J Res US Geol Surv 4:41–47

Arth JG, Barker F (1976) Rare-earth partitioning between hornblende and dacitic liquid and implications for the genesis of trondhjemitic-tonalitic magmas. Geology 4:534–536

Bacon CR (1990) Calc-alkaline, shoshonitic, and primitive tholeiitic lavas from monogenetic volcanoes near Crater Lake, Oregon. J. Petrol 31:135–166

Bagby WC, et al (1981) Contrasting evolution of calc-alkalic volcanic and plutonic rocks of Western Chihuahua, Mexico. J Geophys Res 86:10402–10410

Beard JS, Lofgren GE (1989) Effect of water on the composition of partial melts of greenstone and amphibolite. Science 244:195–197

Beard JS, Lofgren GE (1991) Dehydration melting and water-saturated melting of basaltic and andesitic greenstones and amphibolites at 1, 3 and 6.9 kbar. J Petrol 32:365–402

Bergantz GW (1989) Underplating and partial melting: implications for melt generation and extraction. Science 245:1093–1095

Boily M, et al (1989) Chemical and isotopic evolution of the Coastal Batholith of Southern Peru. J Geophys Res 94:12483–12498

Boynton WV (1984) Cosmochemistry of the rare earth elements: meteorite studies. In: Henderson P (ed) Rare earth element geochemistry. Elsevier, Amsterdam New York, pp 63–114

Burnham CW (1979a) Magmas and hydrothermal fluids. In: Barnes HL (ed) Geochemistry of hydrothermal ore deposits. Wiley Interscience, New York, pp 71–136

Burnham CW (1979b) The importance of volatile constituents. In: Yoder HS (ed) The evolution of the igneous rocks–fiftieth anniversary perspectives. Princeton Univ. Press, Princeton, pp 439–482

Carroll MR, Wyllie PJ (1990) The system tonalite-H_2O at 15 kbar and the genesis of calc-alkaline magmas. Am Mineral 75:345–357

Chappell BW, White A (1974) Two contrasting granite types (expanded abstract). Pacific Geol 8:173–174

Chappell BW, et al (1987) The importance of residual source material (restite) in granite petrogenesis. J Petrol 28:1111–1138

Clemens JD, Vielzeuf D (1987) Constraints on melting and magma production in the crust. Earth Planet Sci Lett 86:287–306

Conrad WK, Kay RW (1984) Ultramafic and mafic inclusions from Adak Island: crystallization history, and implications for the nature of primary magmas and crustal evolution in the Aleutian Arc. J Petrol 25:88–125

Crock JG, et al (1986) Separation and preconcentration of the rare-earth elements and yttrium from geological materials by ion-exchange and sequential acid elution. Talanta 7:601–606

Czamanske GK, Wones DR (1973) Oxidation during magmatic differentiation, Finnmarka Complex, Oslo area, Norway: part 2, the mafic silicates. J Petrol 14:349–380

DePaolo DJ (1981) A neodymium and strontium isotopic study of the Mesozoic calc-alkaline granitic batholiths of the Sierra Nevada and Peninsular Ranges, California. J Geophys Res 86:10470–10488

Dilles JH (1987) Petrology of the Yerington batholith: evidence for evolution of porphyry copper ore fluids. Econ Geol 82:1750–1789

Dodge FCW, et al (1982) Compositional variations and abundances of selected elements in granitoid rocks and constituent minerals, Central Sierra Nevada Batholith, California. USGS Prof Pap 1248

Eggins S, Hensen BJ (1987) Evolution of mantle-derived, augite-hypersthene granodiorites by crystal-liquid fractionation: Barrington Tops batholith, eastern Australia. Lithos 20:295–310

Eggler DH (1972) Amphibole stability in H_2O-undersaturated calc-alkaline melts. Earth Planet Sci Lett 15:28–34

Engles JC, et al (1976) Summary of K-Ar, U-Pb, Pb-alpha, and fission track ages of rocks from Washington state prior to 1975 (exclusive of Columbia Plateau basalts). USGS Misc Field Studies Map MF-710

Erickson EH Jr (1977) Petrology and petrogenesis of the Mount Stuart batholith–plutonic equivalent of the high alumina basalt association? Contrib Mineral Petrol 60:183–207

Farmer GL, DePaolo DJ (1983) Origin of Mesozoic and Tertiary granite in the western United States and implications for pre-Mesozoic crustal structure 1: Nd and Sr isotopic studies in the geocline of the northern Great Basin. J Geophys Res 88:3379–3401

Fountain JC, et al (1989) Melt segregation in anatectic granites: a thermo-gravitational model. J Volcanol Geotherm Res 39:279–296

Fujimaki H, et al (1984) Partition coefficients of Hf, Zr, and REE between phenocrysts and groundmasses. J Geophys Res 89:B662–B672

Green TH, Pearson NJ (1985) Rare earth element partitioning between clinopyroxene and silicate liquid at moderate to high pressure. Contrib Mineral Petrol 91:24–36

Gromet LP, Silver LT (1987) REE variations across the Peninsular Ranges batholith: implications for batholithic petrogenesis and crustal growth in magmatic arcs. J Petrol 28:75–125

Hammarstrom JM, Zen E-An (1986) Aluminum in hornblende: an empirical geobarometer, Am Mineral 71:1297–1313

Harrison TM, Watson EB (1984) The behaviour of apatite during crustal anatexis: equilibrium and kinetic considerations. Geochim Cosmochim Acta 48:1467–1477

Helz RT (1976) Phase relations of basalts in their melting ranges at P_{H_2O} = 5 kbar, part II: melt compositions. J Petrol 17:139–193

Hildreth W, Moorbath S (1988) Crustal contributions to arc magmatism in the Andes of Central Chile. Contrib Mineral Petrol 98:455–489

Hill RI (1988) San Jacinto intrusive complex 1: geology and mineral chemistry, and a model for intermittant rechange of tonalitic magma chambers. J Geophys Res 93:10325–10348

Holloway JR, Burnham CW (1972) Melting relations of basalt with equilibrium water pressure less than total pressure, J Petrol 13:1–29.

Huang WL, Wyllie PJ (1986) Phase relationships of gabbro-tonalite-granite-water at 15 kbar with applications to differentiation and anatexis. Am Mineral 71:301–316

Irving AJ, Frey FA (1984) Trace element abundances in megacrysts and their host basalts: constraints on partition coefficients and megacryst genesis. Geochim Cosmochim Acta 48:1201–1221.

Kilinc IA, Burnham CW (1972) Partitioning of chloride between a silicate melt and coexisting aqueous phase from 2 to 8 kilobars. Econ Geol 67:231–235

Kistler RW, et al (1986) Isotopic variation in the Tuolumne Intrusive Suite, central Sierra Nevada, California. Contrib Mineral Petrol 94:205–220

Le Bel L, et al (1985) A high-K, mantle derived plutonic suite from 'Linga', near Arequipa (Peru). J Petrol 26:124–148

LeMaitre RW (1989) A classification of igneous rocks and glossary of terms. Blackwell Scientific, Oxford

Luhr JF, Carmichael ISE (1980) The Colima volcanic complex, Mexico. Contrib Mineral Petrol 71:343–372

Misch P (1966) Tectonic evolution of the northern Cascades of Washington state. In:Gunning HC (ed) Tectonic history and mineral deposits of the western Cordillera. Can Inst Min Metall 8:pp 101–148

Mooney WD, Weaver CS (1989) Regional crustal structure and tectonics of the Pacific Coastal states; California, Oregon, and Washington. In: Pakiser LC, Mooney WD (eds) Geophysical framework of the continental United States. GSA Mem 172: pp 129–162

aney MT (1983) Phase equilibria of rock-forming ferromagnesian silicates in granitic systems. Am J Sci 283:993–1033

oyes HJ, et al (1983) A tale of two plutons: geochemical evidence bearing on the origin and differentiation of the Red Lake and Eagle Peak plutons, central Sierra Nevada, California. J Geol 91:487–509

Perfit MR, et al (1980) Trace element and isotopic variations in a zoned pluton and associated volcanic rocks, Unalaska Island, Alaska: a model for fractionation in the Aleutian calcalkaline suite. Contrib Mineral Petrol 73:69–87

Pitcher WS (1987) Granites and yet more granites forty years on. Geol Rundsch 76:51–79

Reid JB, et al (1983) Magma mixing in granitic rocks of the Central Sierra Nevada, California. Earth Planet Sci Lett 66:243–261

Richards TA (1971) Plutonic rocks between Hope, B.C., and the 49th Parallel (unpubl). PhD dissertation, Univ British Columbia

Rushmer T (1991) Partial melting of two amphibolites: contrasting experimental results under fluid absent conditions. Contrib Mineral Petrol 107:41–59

Rutter MJ, Wyllie PJ (1988) Melting of vapour-absent tonalite at 10 kbar to simulate dehydration-melting in the deep crust. Nature 331:159–160

Takahashi E (1986) Genesis of calc-alkali andesite magma in a hydrous mantle-crust boundary: petrology of lherzolite xenoliths from the Ichinomegata crater, Oga Peninsula, northeast Japan, part II. J Volcanol Geotherm Res 29:355–395

Tepper JH (1991) Petrology of mafic plutons and their role in granitoid genesis, Chilliwack batholith, North Cascades, Washington (unpubl). PhD dissertation, Univ of Washington

Ulmer P (1989) The dependence of the Fe^{2+}-Mg cation-partitioning between olivine and basaltic liquid on pressure, temperature, and composition. Contrib Mineral Petrol 101:261–273

Walawender MJ, Smith TE (1980) Geochemical and petrologic evolution of the basic plutons of the Peninsular Ranges batholith, southern California. J Geol 88:233–242

Watson EB, Green TH (1981) Apatite/liquid partition coefficients for the rare earth elements and strontium. Earth Planet Sci Lett 56:405–421

Wolf MB, Wyllie PJ (1989) The formation of tonalitic liquids during the vapor-absent partial melting of amphibolite at 10 kbar. Eos 70:506

Wyllie PJ, et al (1976) Granitic magmas: possible and impossible sources, water contents, and crystallization sequences. Can J Earth Sci 13:1007–1019